Transition from ciliary to flapping mode in a swimming mollusc: flapping flight as a bifurcation in Re_ω

By STEPHEN CHILDRESS[1] and ROBERT DUDLEY[2]

[1]Applied Mathematics Laboratory, Courant Institute of Mathematical Sciences, New York University, 251 Mercer Street, New York, NY 10012, USA

[2]Department of Integrative Biology, University of California, Berkeley, Berkeley, CA 94720-3140, USA

From observations of swimming of the shell-less pteropod mollusc *Clione antarctica* we compare swimming velocities achieved by the organism using ciliated surfaces alone with velocities achieved by the same organism using a pair of flapping wings. Flapping dominates locomotion above a swimming Reynolds number Re in the range 5–20. We test the hypothesis that $Re \approx 5$–20 marks the onset of 'flapping flight' in these organisms. We consider the proposition that forward, reciprocal flapping flight is impossible for locomoting organisms whose motion is fully determined by a body length L and a frequency ω below some finite critical value of the Reynolds number $Re_\omega = \omega L^2 / \nu$. For a self-similar family of body shapes, the critical Reynolds number should depend only upon the geometry of the body and the cyclic movement used to locomote. We give evidence of such a critical Reynolds number in our data, and study the bifurcation in several simplified theoretical models. We argue further that this bifurcation marks the departure of natural locomotion from the low Reynolds number or Stokesian realm and its entry into the high Reynolds number or Eulerian realm. This occurs because the equilibrium swimming or flying speed U_f obtained at the instability is determined by the mechanics of a viscous fluid at a value of $Re_f = U_f L / \nu$ that is not small.

1. Introduction

Because of the difficulty of treating complex time-dependent geometries, theories of natural locomotion in fluids generally utilize either low Reynolds number approximations, applicable to micro-organisms, or the assumptions of inviscid fluid dynamics supplemented by boundary-layer theory, applicable to insects, birds, and fish. These two regimes are also distinct in terms of the observed mechanisms of locomotion (Lighthill 1975; Childress 1981*a*; Dudley 2000). Reduced to its simplest terms, locomotion in the Stokesian or low Reynolds number realm relies on the diffusion of momentum, while that in the Eulerian or high Reynolds number realm emphasizes the advection of momentum in highly structured vortical fields. In the former, one thinks of non-reciprocal, cyclic boundary movements which can steadily locomote the organism, whereas in the latter one envisages mechanisms for producing thrust and lift through vortex shedding and interactions of the organism and its appendages with the shed vorticity.
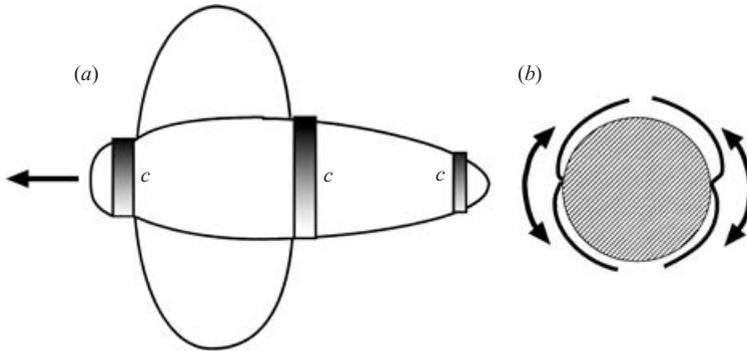
FIGURE 1. Sketch of *Clione antarctica* (typical length 6 mm) indicating three bands of cilia (*c*) and the extended wings (pteropodia). Extreme positions of wings against body as sketched from video, flapping frequency 2.25 cycles s^{-1}. (*a*) Ventral perspective, the arrow indicating the direction of body movement, and *c* the ciliary bands. (*b*) Anterior perspective.

However, numerous taxa locomote at characteristic Reynolds numbers in the range 1–100, corresponding purely to neither the Stokesian nor the Eulerian realm. A broad diversity of aquatic invertebrate taxa (e.g. representatives in Crustacea, Chaetognatha and other vermiform phyla, Mollusca, some larval as well as adult Insecta), as well as many small flying insects, operate at such *intermediate* Reynolds numbers (e.g. Walker 2002; McHenry, Azizi & Strother 2003). Equally important, many taxa transit ontogenetically across this range (e.g. larval fish, many marine invertebrate larvae). Such ontogenetic shifts mandate either loss of locomotor mechanisms (e.g. settling in taxa that are sessile as adults) or their functional transformation. The mechanisms of locomotion appropriate to this Reynolds number range thus do not fall fully within the scope of either Stokesian or Eulerian theory, although presumably the fluid mechanics is adequately described by solutions of the unapproximated Navier–Stokes equations. What can be established with certainty (see the discussion of §3) is that reciprocal motions associated with the Eulerian realm, the simple up-and-down movement of a flapping wing in forward flight, for example, fails to locomote in the Stokesian realm. (We discuss below the meaning of reciprocal motion.) Thus, the intermediate Reynolds number range is not only one where ciliary and flagellar mechanisms give way to flapping flight, but also one in which reciprocal flapping becomes a useful alternative.

The present discussion has been motivated by the opportunity we had in November and December of 2000, while carrying out field work at McMurdo Station, Antarctica, to observe the swimming behaviour of the pteropod *Clione antarctica*. These small gastropod molluscs, which can be found in the waters beneath the ice of McMurdo Sound, are equipped not only with bands of cilia but also with a pair of wings (figure 1). As a result, they have two distinct modes of swimming. In *ciliary mode* the wings are retracted into the body and the swimming is by metachronal waves of movement around three bands of cilia encircling the body. The ciliary mechanism is effective for locomotion at arbitrarily small Reynolds numbers. In *flapping mode*, the wings are extended and flapped, the sequence of wing positions being indicated qualitatively in figure 1. Although the organism is swimming, this mode, when effective, can be appropriately described as 'forward flapping flight'. We remark that these specimens were not fully developed adults, and it should be understood that all our results pertain to an early developmental stage of *Clione antarctica*.

While in flapping mode, movements of cilia could often still be seen, to a degree which varied considerably across the organisms studied, but our working hypothesis is that some slight ciliary activity was always present. Remarkably, in experiments described in the next section, we found that it was possible (at least for over two dozen of the organisms we studied) to induce three distinct behaviours: the two swimming modes just described, and a *drift mode* in which neither of the organelles were used and the organism drifted under its natural buoyancy. (The drift mode was important as a reference since these organisms can modify somewhat their natural buoyancy.) It thus became possible to test the hypothesis that there should be some transitional values of parameters determining when a flapping mode becomes more effective to the organism than the ciliary mode, as measured by the absolute speed of swimming. As we shall indicate below, the data are consistent with a hypothesis that the swimming Reynolds number in flapping mode exceeds that of the ciliary mode at values of *Re* of approximately 5–20 based on body length and swimming speed.

In the present paper we shall describe these measurements of 'bi-modal' swimming, and then, using simplified analytical models, one based upon Oseen's approximate equations of motion for a viscous fluid, another based upon a periodic array of flapping wings, test the hypothesis that flapping structures should cease to be effective in the production of thrust below a Reynolds number consistent with our observations.

Because of this failure of reciprocal flapping in the Stokesian realm, it is tempting to assert that, for a given locomoting organism executing fixed reciprocal motions, there must exist a fluid viscosity above which forward flapping flight becomes impossible. The relative effectiveness of ciliary and flapping modes is a complex issue, involving aspects of behaviour over which one has no control experimentally. There are however several questions which the above assertion raises: (i) How can this critical viscosity be translated into transitional values for the dimensionless parameters of the system, from ciliary to flapping modes? (ii) How can this proposition be tested by our observations of pteropod locomotion, when and if ciliary propulsion is also present in the flapping mode? (iii) Can models of reciprocal flapping be found which exhibit the bifurcation from rest to locomotion as viscosity is decreased, and which are consistent with the observations?

Our primary goal in this paper will be to argue that the transition to flapping flight actually occurs as a mathematical bifurcation with respect to a flapping Reynolds number. That is, locomotion using reciprocal flapping can be regarded as resulting from the instability of the system of the flapping body and the fluid medium, initiated by a 'push' of the immobile flapping body, and 'saturated' in the state of forward flight. Our discussion will refer to three distinct Reynolds numbers: $Re_{c,f} = U_{c,f} L/\nu$ being the swimming Reynolds numbers in ciliary or flapping modes, L being body length; and $Re_\omega = \omega L^2/\nu$, a Reynolds number pertinent only to the flapping mode. Re_ω will be our bifurcation parameter. The derived frequency parameter $\sigma = U_f/\omega L = Re_f/Re_\omega$ will also be useful. The parameter Re_ω is distinguished by being characteristic of a flapping body quite apart from whether or not locomotion occurs, whereas $Re_{c,f}$ are derived parameters.

The paper is organized as follows: in the next section we summarize our *Clione* data and examine it for evidence of transition and criticality. In §3 we discuss the general proposition of bifurcation to flapping flight in terms of the dimensionless parameters and compare transitional swimming with the concept of a critical Reynolds number. In §§4, 5, and 6 we consider several two-dimensional models of bifurcation to flapping flight. Some general aspects of the bifurcation, and how it might be studied as a

three-dimensional Navier–Stokes calculation, are considered in §7. Finally, in §8 we summarize our results and discuss their relation to other problems and questions.

It is important to emphasize that, throughout this paper, we use the term 'reciprocal' in the context of low-Re fluid mechanics, e.g. Batchelor (1967); Lighthill (1975); Purcell (1977); Childress (1981*a*). To define reciprocal motion, suppose that the flapping mode consists of a periodic cycle through an ordered sequence of configurations, a configuration being the set of points which instantaneously defines the surface of the body. In reciprocal motion, this ordered sequence is indistinguishable from the sequence obtained under time reversal of the flapping cycle. Thus a scallop, which opens slowly and closes quickly, while in each case moving through the same configurations, is a reciprocal swimmer. A reciprocal motion is identical under a simultaneous one–one mapping and reversal in the direction of the time variable. (The flexibility in timing of a movement will be useful to us in devising a tractable analytical model.)†

Of course reciprocity of the motion does not guarantee that the organism will locomote in any fluid, a situation which would imply an infinite critical Reynolds number. Note also that we refer here to the configurations determined in free locomotion of the body. In natural swimming and flying, the configuration of a flapping body will in general depend upon the flow field which surrounds it, as the body tissue reacts to the forces imposed by the fluid. In our discussion, when referring to a untethered 'reciprocal flapper', we shall mean an organism executing a fixed reciprocal motion while in free locomotion.

Finally, we stress that our focus on reciprocal motions is not meant to imply that such motions are omnipresent in biology. On the contrary, most natural locomotion seems to involve some non-reciprocity derived kinematically or morphologically. However, by looking closely at the implications of reciprocity, we are able to isolate a bifurcation which we suggest underlies the relative advantages of flapping flight, even when some non-reciprocal motions are present.

2. Observations of swimming by *Clione antarctica*

Pteropods were collected using plankton nets, primarily through holes in the sea ice near McMurdo Station, Ross Island, Antarctica. Sampling depths ranged from 10 to 60 m. Specimens were kept in seawater in a holding tank, where they would remain active for up to four days. Our measurements of swimming velocity were performed in an open cylindrical glass tank of radius 6 cm and height 9 cm. This tank was immersed in a temperature-controlled water bath. The interior of the experimental tank was fitted with a conical paper structure to facilitate placement of the pteropod at the bottom of the tank. Pteropods would then ascend to the water's surface. A mirror oriented at 45° to the horizontal was used to record lateral views with a digital video camera, which also recorded ascent from a top perspective. The (small) velocity component normal to the plane of view could not be measured and was set to zero in our data analysis. Video images were analysed to obtain head and tail positions at two distinct times during a phase of swimming in flapping or ciliary mode, or of buoyant drift, as well as the frequency of wing beating in flapping mode.

---

† There are generalizations of this reciprocity concept, involving symmetry operations other than time reversal, which leave the fluid-dynamical problem invariant. An example is mirror symmetry of the boundary motion, realized say by the circular movement of a straight filamentary appendage so that it sweeps out the surface of a cone.

Runs in all three locomotion modes were recorded at water temperatures of approximately $-2\,°C$, $0\,°C$, and $+2\,°C$, to examine the effect of temperature-based viscosity change. The above runs were then repeated in seawater for which viscosity had been modified by the addition of dextran, a high molecular weight carbohydrate (average molecular weight 24500). Using falling ball viscometry, the fluid viscosity could be estimated as $(1.886 - 0.0595T)(1 + 1.3c)$, where T is temperature in $°C$ and c is the dextran concentration as a percentage of weight. Most runs were at the concentrations $c = 0$ and 0.1. Thus viscosity varied by about 13% through separate variations of temperature and dextran concentration. While relatively small, this variation represents what occurs naturally for these organisms owing to small temperature variation in the polar environment. The larger variation of the observed swimming Re came from the experimental range of body sizes and swimming speeds.

We now describe the reduction of our data to obtain Re based upon body length and speed of swimming. The latter was taken as the speed of the centre of the line segment joining the point designated as the head to that designated as the tail. Let y be the vertical coordinate, and x the horizontal coordinate in the plane of observation. Upward drift velocities were dominated by the y-component and this was subtracted from the y-component of velocity in cilia or flapping mode, to obtain a 'buoyancy-corrected' swimming speed. The rationale for this depends upon the locomotion mode. In flapping mode, we may regard the wings as generating thrust and thus adopt an Eulerian view. In quasi-steady linearized airfoil theory, thrust is proportional to the square of the flapping frequency, but is independent of the speed of locomotion. If the approach speed is augmented by buoyancy, this gives a hydrodynamically unwanted contribution which must be subtracted out. In ciliary mode, we adopt the Stokesian view of envelope theory (see Blake 1971), which equates the effect of the ciliated band to an effective 'slip' velocity at its outer extremity, and this velocity locally replaces the no-slip condition at the body. The steady ciliary swimming velocity is that velocity which makes the force on the body equal to zero when the flow is determined using the modified boundary condition. The effect of a buoyancy force on this flow is to increment the swimming speed in order to maintain force equilibrium, and this increment must be subtracted to obtain the ciliary swimming speed of a neutrally buoyant body. Of course, the actual Re range here is intermediate and we shall see that fully unsteady conditions prevail, so that neither argument is exactly applicable. Since the buoyancy correction is approximate, we shall exhibit uncorrected data as well.

For each locomotion mode, three sets of kinematic measurements per individual were made at each combination of temperature and viscosity. Final results for the three runs under given conditions of locomotion mode, T, and c were averaged, yielding a set of pairs (Re_f, Re_c) of the swimming Reynolds numbers in flapping and ciliary mode for different individuals, temperatures, and dextran concentrations. For the buoyancy-corrected data we plot these pairs and the associated linear regression, in figure 2. The corresponding data uncorrected for buoyancy is shown in figure 3.

The $45\,°$ line in figures 2 and 3 would be the locus of points if flapping and ciliary modes were equally effective at all Reynolds numbers. The data, however, clearly indicate that swimming is faster in flapping mode for sufficiently high Re. At lower Re, we offer two distinct possibilities. (a) If flapping mode is additive, in the sense that ciliary activity is undiminished as the wings flap, the data should be close to the $45\,°$ line below some value of Re. (b) If flapping mode implies no ciliary activity, the data should tend to (0,0) along a curve well above the $45\,°$ line. The considerable scatter of the data reflects the uncertainty of buoyancy corrections, out-of-plane velocity
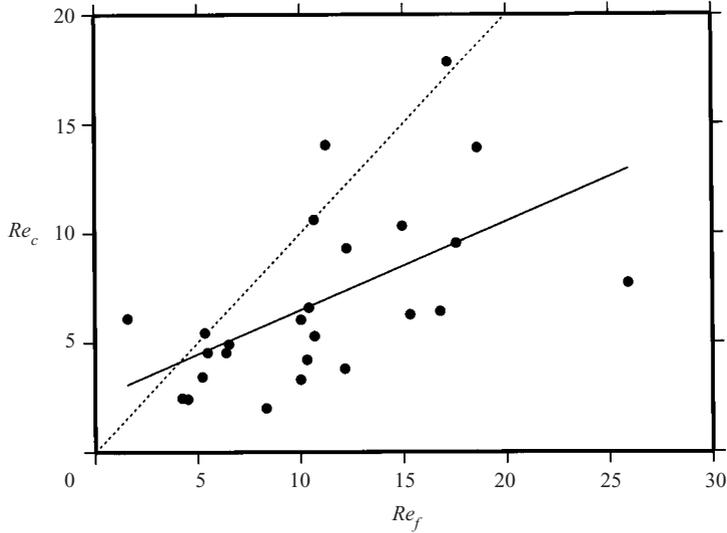
FIGURE 2. R_c versus R_f for swimming of *Clione antarctica*, averaged data corrected for buoyancy. The dashed line is the line $Re_c = Re_f$.
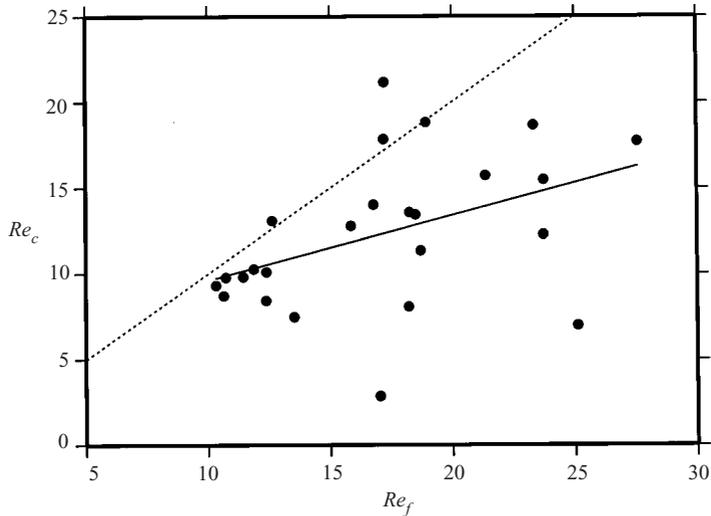

FIGURE 3. R_c versus R_f for swimming of *Clione antarctica*, averaged data uncorrected for buoyancy. The dashed line is the line $Re_c = Re_f$.

components, and possible contributions from ciliary activity in flapping mode. But the most important source of error is probably the behavioural variability of the pteropods themselves.

We pass immediately to a different presentation of the data most relevant to the subject of the present paper. In figure 4 we show the observed Re_f, using a swimming velocity corrected for buoyancy, versus Re_ω. In order to focus on the lower Re, we have discarded all data points lying outside the rectangle of figure 4. The data strongly suggest a critical value of Re_ω, denoted now by $Re_{\omega c}$, of close to 12. The indication is that Re_f is more strongly correlated with Re_ω that with Re_c.
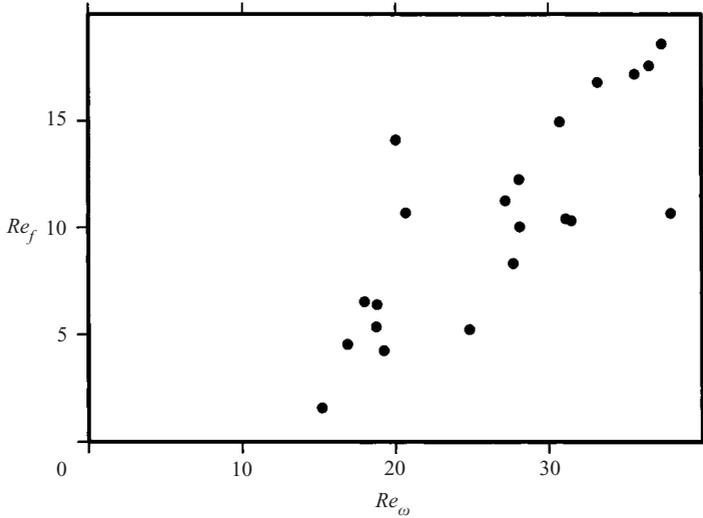
FIGURE 4. Buoyancy-corrected Re_f as a function of $Re_\omega = \omega L^2/\nu = Re_f/\sigma$.
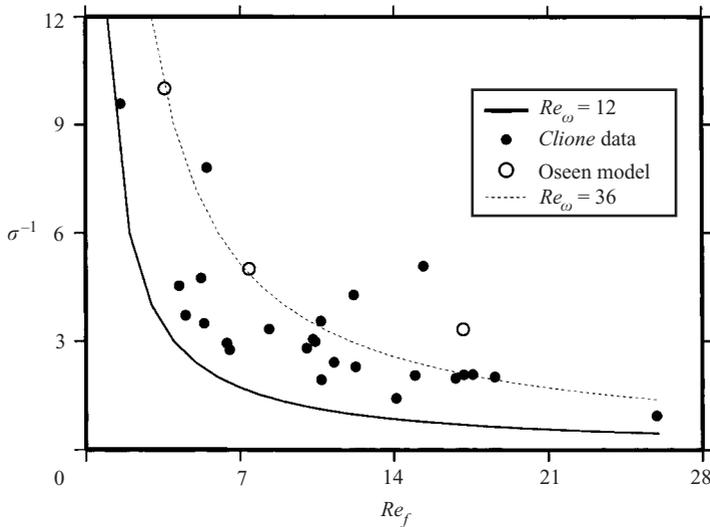

FIGURE 5. The solid circles are values of σ^{-1} and Re_f from observations of the flapping mode of *Clione antarctica*. Both parameters are corrected for buoyancy. The open circles are for the model of §4.2, computed with $k = 10$, $N = 10$, and $L = 1$. The solid line is the hyperbola $Re_\omega = 12$, and the dashed line is the hyperbola $Re_\omega = 36$.

Although figure 4 is the natural representation of a bifurcation to 'flapping flight', we were initially interested in the transition from cilial to flapping locomotion, and hence on the presentation of figures 2 and 3. We were led to consider the transition as a bifurcation with respect to Re_ω by the following observation. If all the pteropods, as well as their swimming movements, were geometrically similar, and if indeed the only dimensionless parameters for the flapping mode were Re_f and $\sigma = Re_f/Re_\omega$, then we should expect that equilibrium swimming speed would be determined by a curve in the (Re_f, σ^{-1})-plane. In figure 5 we plot the *Clione* data in this way, both parameters being corrected for buoyancy. It was noted that the data seemed to lie
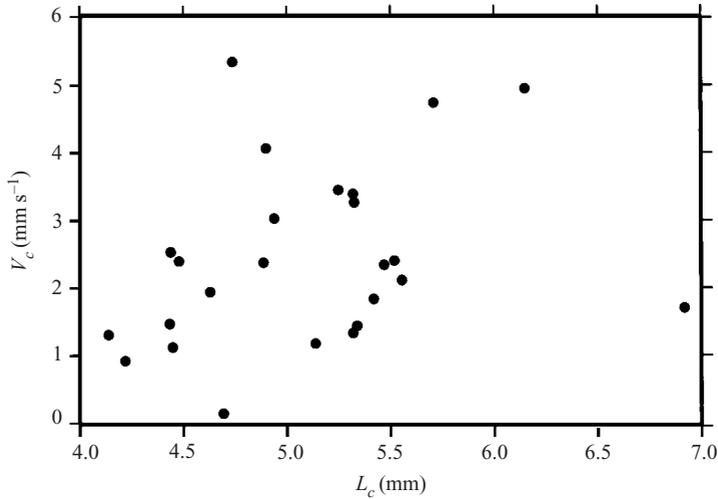
FIGURE 6. Scatter plot of swimming speed versus body size in ciliary mode.

above a hyperbola: $Re_\omega = \text{constant} > 0$. This representation of the data, which brings in Re_ω explicitly for the first time, gave the first indication of the existence of a minimum or critical value of Re_ω for locomotion by reciprocal flapping. Indeed, $Re_{\omega c}$ determines the hyperbola which approximates the curve of equilibrium swimming speed in the limit of small Re. The hyperbolae shown in figure 5 in fact correspond to the observed and model values of $Re_{\omega c}$.

Perhaps the most important question concerning these observations is to what degree the flapping mode of *Clione* is in fact reciprocal. We often saw slight lateral undulations of the body in flapping mode, and the response of flexible bodies to oscillating fluid forces is usually not reciprocal. We should note also that the wing motion depicted in figure 1 involves considerable 'body slapping', particularly at the bottom of the downstroke. It is important to point out in this connection that, while motion effective in the Stokesian realm must be non-reciprocal, many non-reciprocal motions also are not effective there. A flexible wing executing movements with complete fore-and-aft symmetry is an example of this. We might well have expanded the class of reciprocal flappers to include all unspecified ineffective movements, without altering the conclusions drawn in §§ 3 and 7.

In spite of these and other sources of experimental error and deviation from the ideal experiment underlying the above arguments, we take these data as evidence of a critical value of Re_ω for *Clione antarctica*.

We suggest that the correlation in figure 4, as opposed to figures 2 and 3, can be traced to the variability of the swimming velocities in ciliary mode. We show in figure 6 the raw data for the buoyancy-corrected swimming speed in ciliary mode versus body length in ciliary mode. The scatter indicates a large variability of the individual level of ciliary activity. Models of locomotion using ciliated surfaces (assumed to occupy a fixed fraction of body surface) show that swimming speed is proportional to $\Omega K a^2$ where Ω, K are a frequency and wavenumber associated with the metachronal waves, and a is a wave amplitude (Brennen 1975). It is not clear how these parameters scale with body size. Figures 2–5 do suggest that the variability of the data resides in the ciliary mode, and that the flapping mode becomes the more effective mode as the swimming Reynolds number increases through the observed range.

3. Transition and criticality in flapping flight

The starting point for our discussion of bifurcation to flapping flight will be the basic result that reciprocal motions cannot locomote in creeping flow, that is, in the Stokesian realm. Having the image of a scallop opening and closing in a sequence of configurations invariant under time reversal, we follow Purcell (1977) and refer to our version of this result as the

Scallop theorem: *If a flapper locomotes at arbitrarily small values of Re_f and Re_ω, its motion cannot be reciprocal.*

As far as we know there has been no rigorous proof of this theorem based upon the mechanics of a Navier–Stokes fluid and free-swimming body. An informal demonstration of the result rests upon the fact that time is a parameter in the Stokesian realm, a given body displacement producing an instantaneous corresponding displacement of all points of the fluid. As the body cycles through configuration space, the centre of volume cycles through displacements. The net displacement obtained over one cycle changes sign under time reversal. Thus, if the motion is reciprocal, this net displacement must be identically zero.

The existence of a critical value of Re_ω follows as a corollary to the scallop theorem.

Corollary: *By changing the frequency ω of a given reciprocal flapper, let the swimming Reynolds number Re_f be observed as a function of Re_ω. Then there is a positive number $Re_{\omega c}$ such that $Re_f(Re_\omega) = 0$ if $Re_\omega < Re_{\omega c}$.*

We give an equally informal proof of the corollary, by first imagining an experiment involving tethered flappers. Consider a collection of self-similar, reciprocal flappers, each characterized by a length L and a frequency ω, and tethered in a uniform stream of velocity U. By 'tether' we mean that the body neither translates nor rotates, and flapping continues unabated as it is held in place.

Assume that there exist values of Re and Re_ω for which the time-averaged force required to hold the organism in place points downstream, that is, net thrust is generated. If the frequency of flapping is now decreased, so that Re_ω is decreased while Re is held fixed, the mean force required to hold the organism must eventually be directed into the oncoming stream, that is to say a drag is experienced, since the motion becomes quasi-steady and the drag is essentially that of a static body. Assuming a continuous dependence of force on Re_ω, there must exist a value of Re_ω where the force vanishes for this Re, thus establishing conditions for equilibrium. Repeating this experiment for all $Re > 0$, we construct a set of pairs (Re_ω, Re_f) for zero force.

For untethered flappers we may perform a similar experiment. We may assume that orientation is such that direction of motion is fixed and $Re_f \geqslant 0$. For suitable initial conditions, we assume that each flapper achieves a unique equilibrium speed. We thus envisage an infinite set S of pairs (Re_ω, Re_f) for equilibrium locomotion, defined for $Re_\omega > 0$. Some of these may now involve a zero value of Re_f.

To prove the corollary we consider

$$r = \inf_S \{Re_\omega | Re_f > 0\}. \tag{3.1}$$

If $r = 0$, there must be an infinite sequence of pairs $(Re_{\omega k}, Re_{fk})$, $k = 1, 2, \ldots$, with $Re_{\omega k} \to 0$ as $k \to \infty$, where locomotion is observed. But then we must also have $Re_{fk} \to 0$ since otherwise we would have observed a finite speed of locomotion for arbitrarily small values of Re_ω, which is unphysical.

Thus, if r were zero, we have established that swimming would occur in the Stokesian realm $Re_\omega, Re_f \ll 1$. By the scallop theorem, the motion cannot be reciprocal, which is a contradiction. Thus $r \equiv Re_{\omega c} > 0$ and necessarily $Re_f = 0$ if $Re_\omega < Re_{\omega c}$. This establishes the corollary.

The precise form of the (Re_ω, Re_f) variation is largely unexplored in the range of Reynolds numbers of interest to us here. Referring now to *Clione antarctica*, the body moves in ciliary mode through the combination of movements of individual cilia, and since these are not individually reciprocal (Lighthill 1975; Childress 1981*a*), the same can be said for the body motion as a whole. The organism then swims at a speed which depends upon the form of the cilia movements, their distribution over the body, and upon the structure of the metachronal waves of cilia activity. The essential point is that swimming occurs in fluids of arbitrarily large viscosity, assuming only that the body movements can be maintained.

It is somewhat simpler conceptually to imagine that the cilia execute identical movements with a fixed frequency ω_{cil}, which has no relation to the frequency ω of the wings, and is typically larger by a factor of 5–10 than the flapping frequency of 1–2 Hz that we observed for *Clione*. The swimming is then such that the advance through the fluid over each cycle of motion is the same. Thus, there is a constant K such that $Re_c = K Re_{\omega cil}$ provided $Re_{\omega cil} \ll 1$.

For the case of the flapping mode, we can compare the situation where the wing movement is not reciprocal to the ciliary mode, for then the advance at small Reynolds number will again obey a scaling $Re_f = K Re_\omega$ for some K. Thus the key point is that such a relation either holds, in which case the motion is not reciprocal, or else it does not and a positive critical Reynolds number exists.

Note that we have not excluded the possibility that at some values of Re_ω exceeding the critical value the rest state might again be globally asymptotically stable. We have also not excluded the possibility that the instability may be subcritical, and a finite 'push' might lead to locomotion at values of Re_ω below the (linear) critical value $Re_{\omega c}$. However there will be a smallest value of $Re_\omega(Re_f)$, $Re_{\omega c}^*$ say, such that if $Re_\omega < Re_{\omega c}^*$ the rest state will be globally asymptotically stable with respect to the starting configuration in the phase space of position and velocity.

The idea of a transition from one mechanism of locomotion to another can be examined in an organism such as *Clione*, having both cilia and wings and the ability to use them independently. We suppose, for the sake of argument, that the two mechanisms are never used simultaneously. Then in ciliary mode, the scaling $Re_c = K Re_{\omega cil}$ holds so long as a Reynolds number associated with the cilia is small. This can be accompanied by values of Re_c of order unity, as is the case observed for *Clione*. Thus, as body size increases and the bifurcation is reached, flapping flight can occur simultaneously with ciliary locomotion and we can refer to transition Reynolds numbers where both modes are accessible, as appears to be the case with *Clione*.

4. Oseenlet models

Since our data indicate that the flapping mode is more effective for the swimming of *Clione* above Re in the range 5–20, it is of interest to examine theoretically the free locomotion of bodies using flapping movements and operating in this range of Re_ω. We shall study a number of simplified models. We should note that every reciprocal flapper has, we claim, a particular value of $Re_{\omega c}$ (perhaps equal to infinity, if the body does not locomote) determined by the geometry of the moving body up to a similarity scaling. A particularly important aspect of this is the degree to which

the body as a whole participates in locomotion, and what part does not participate and contributes only to drag. A direct comparison of the values of $Re_{\omega c}$ obtained in the disparate models we shall examine with those observed for the pteropods is thus neither warranted or useful. Our aim will therefore be simply to verify in each case the existence of a bifurcation.

In the present section we develop a linear theory of forward flapping flight based upon the Oseen approximation. Our object is to illustrate the possibility of locomotion by a flapping force field, and to study the dependence of the process upon the parameters Re_ω and Re_f.

We shall replace the appropriate Navier–Stokes equations by the linear Oseen equations, modified by a damping term,

$$\boldsymbol{u}_t + \sigma \boldsymbol{u}_x + k^{-1}\boldsymbol{u} + \nabla p - \epsilon \nabla^2 \boldsymbol{u} = \boldsymbol{F}, \quad \nabla \cdot \boldsymbol{u} = 0. \tag{4.1}$$

Here we have taken the linearization to be about a dimensionless velocity $\sigma = Re_f/Re_\omega$, and $\epsilon = Re_\omega^{-1}$ where L is an as yet unspecified reference length. We have included in (4.1) an arbitrary force field force $\boldsymbol{F}(\boldsymbol{x}, t)$. We shall restrict our calculations to two dimensions, and allow $\boldsymbol{F}$ to be various distributions of time-dependent point forces. The term $k^{-1}\boldsymbol{u}$ is a non-standard modification equivalent to placing the flow in a porous medium with permeability k. This term is introduced to improve convergence of time integrals which appear below.

A linearization of this kind is of interest for the study of forward flight, where a well-defined free stream makes some sense. Nevertheless, it should be born in mind that it represents a rather drastic simplification of the advection of vorticity, advection by the true velocity having now been replaced by advection with the free stream. This can lead to errors in the position of vorticity shed from the body during active flapping which are reflected in the forces experienced by the body. Also, at higher values of Re, the boundary layers are not correctly described, although for planar surfaces aligned with the free stream the penalty is not too severe.

It is convenient to utilize the following representation of the Oseen response to a point force at the origin at time 0:

$$\boldsymbol{u}_t + \sigma \boldsymbol{u}_x + k^{-1}\boldsymbol{u} + \nabla p - \epsilon \nabla^2 \boldsymbol{u} = \boldsymbol{f}\delta(\boldsymbol{x})\delta(t), \quad \nabla \cdot \boldsymbol{u} = 0, \tag{4.2}$$

where $\boldsymbol{f}$ is a constant vector. With

$$u_i = \left[\delta_{ij}\nabla^2\chi - \frac{\partial^2\chi}{\partial x_i \partial x_j}\right]f_j, \quad p = -\epsilon f_i \frac{\partial\chi}{\partial x_i}, \tag{4.3}$$

we obtain from (4.2) that $\chi = \mathrm{e}^{-t/k}K(\boldsymbol{x} - \sigma t \boldsymbol{i}, t)$, where $K(\boldsymbol{x}, t)$ satisfies

$$\frac{\partial \nabla^2 K}{\partial t} - \epsilon \nabla^4 K = \delta(\boldsymbol{x})\delta(t). \tag{4.4}$$

The general method we shall employ is superposition of fundamental solutions generated by a moving point force. If the right-hand-side of (4.4) is replaced by, for example, $f(t)\boldsymbol{j}\delta(\boldsymbol{x} - \boldsymbol{x}_0(t))$ and we assume that $\chi(\boldsymbol{x}, 0) = 0$ then (4.3) applies with

$$\chi(\boldsymbol{x}, t) = \int_0^t f(\tau)\mathrm{e}^{-(t-\tau)/k}K(\boldsymbol{x} - \boldsymbol{x}_0(\tau) - \sigma(t-\tau)\boldsymbol{i}, t - \tau)\,\mathrm{d}\tau. \tag{4.5}$$

4.1. *Single oscillating Oseenlet*

In two dimensions, we have from (4.4) and the requirement that $K(0, 0, t) = 0$ that

$$K(x, y, t) = \frac{1}{2\pi} \int_0^r \frac{1 - \exp[-s^2/(4\epsilon t)]}{s} \, \mathrm{d}s, \ r = \sqrt{x^2 + y^2}. \tag{4.6}$$

A related classical two-dimensional problem of interest in connection with (4.5) is the calculation of the drag of a circular cylinder in steady flow at low Re, see Lamb (1945, p. 609), as the limit of the time-dependent flow created by impulsive motion. We outline this calculation in appendix A for the undamped Oseen theory.

In the present context we are interested in flapping motions and hence in Oseenlets which are oscillating along lines perpendicular to the free stream. Suppose that a point force of strength $f(t)\boldsymbol{j}$ is positioned at $x = 0$, $y = \sin 2\pi t$. (The reference length L is here taken as the flapping amplitude.) We now ask, taking this point force as a simple 'flapping wing', the following question: what horizontal velocity $U(t)$ is induced at the instantaneous position of the force, and what is the limit for large t of its average over one cycle starting from time t as a function of Re_ω and Re_f? We denote the latter limit by $\langle U \rangle$.

The thrust that occurs in flapping flight would be obtained as a mean upstream component of $U(t)$, the thrust resulting from the resistance presented by the moving body, here represented by a point force. We are interested not so much in the magnitude of an upstream component, but rather in how its magnitude changes as a function of Re_ω and Re_f. The critical curve in (Re_ω, Re_f) space is now defined by zero average body force, or thrust = drag and so $\langle U \rangle = -1$.

We shall assume here that $f(t) = C_f \epsilon 2\pi \cos 2\pi t$, that is, the force is proportional to velocity with a force coefficient $C_f \epsilon$. A force coefficient $\approx 10/Re$ is reasonable for steady flow past a circular cylinder at these intermediate Reynolds numbers. Here we shall choose C_f to be large enough to establish a convenient critical value of Re_ω. In effect we are considering a fictitious body of sufficiently high drag to allow the study of locomotion in this linear model.

We then have the explicit expression

$$\langle U(t) \rangle = -\frac{2C_f}{Re_\omega} \left\langle \int_0^t \cos 2\pi\tau \, \frac{XY}{R^4} \mathrm{e}^{(\tau-t)/k} [1 - (1 + N)\mathrm{e}^{-N}] \, \mathrm{d}\tau \right\rangle, \tag{4.7}$$

where $X = \sigma(t - \tau)$, $Y = \sin 2\pi t - \sin 2\pi\tau$, $R^2 = X^2 + Y^2$, $N = Re_\omega R^2/[4(t - \tau)]$. The time integral is convergent at $\tau = t$, and as $\epsilon \to 0$ is dominated by the contribution there and has a finite limit. Note that the damping term $\mathrm{e}^{(\tau-t)/k}$ assists convergence at large t by decreasing the influence of distant wake vorticity.

We show in figure 7 the result of calculations with values $C_f = 41, k = 2.5$, which makes $Re_{\omega c} = 5$. The critical curve is shown. We thus may conclude that an oscillating vertical point force provides a simple qualitative model of flapping flight illustrating bifurcation from the state of rest. The shape of this surface is a result of advection (with the free-stream velocity) of the vortical component of the Oseen solutions. At higher Reynolds numbers this component lies at any time in the vicinity of a sinusoidal curve extending downstream from the position of the oscillating point. The summed effect of these vortices at the point determines $U(t)$. As Re decreases, this vortical structure becomes more diffuse and U diminishes.

4.2. *Approximate two-dimensional wing model*

We consider a calculation which develops further the representation of oscillating point forces in the Oseen model. Our goal is to approximately calculate the force
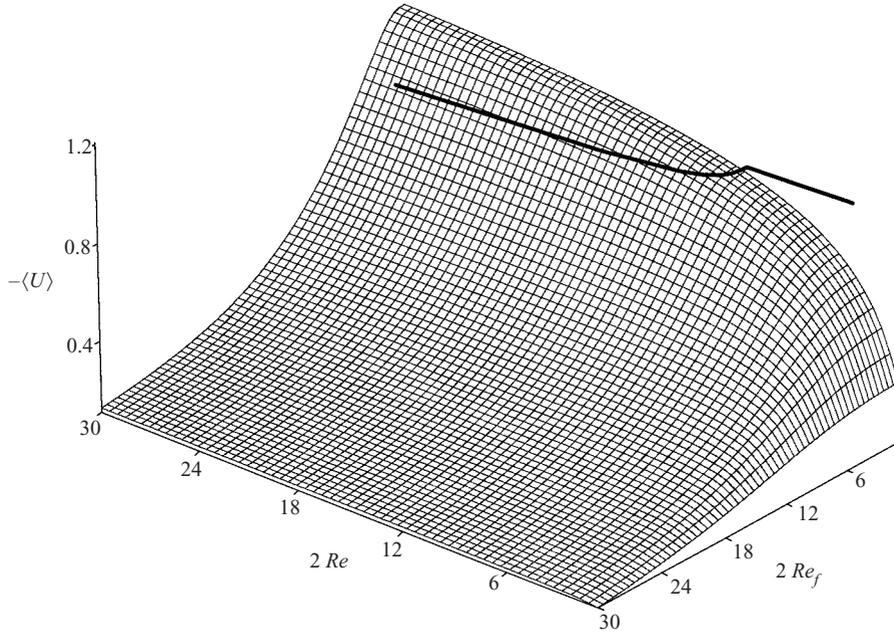
FIGURE 7. Surface plot of $-\langle U \rangle$ as a function of $2Re_\omega$ and $2Re_f$ for an oscillating Oseenlet with position $u = \sin 2\pi t$, see §4.1 The damped Oseen model is used here with $k = 2.5$. The drag coefficient is set to make $Re_{\omega c} = 5$. Bifurcation to flapping flight occurs when $\langle U \rangle = -1$. The function $Re_f(Re_{\omega c})$ is indicated by a solid line, representing the intersection of the surface with the plane $-\langle U \rangle = 1$.

rather than to simply impose it. We make use of N identical point forces, uniformly distributed in the interval $I : 0 \leqslant x \leqslant L$, all at vertical position $y = \sin \omega_w t$. (Again the reference length is taken as the flapping amplitude.) We assume identical forces of the form $\boldsymbol{F} = 2\pi f_0 \cos 2\pi t \, \boldsymbol{j}$ with f_0 a free parameter. We choose f_0 by the condition that the coefficient of the $\cos 2\pi t$ harmonic, of the instantaneous spatial average over I of the vertical velocity component, be equal to the maximum vertical velocity 2π of the point forces. This is an approximate attempt to partially satisfy boundary conditions on a solid planar surface.

We define $\overline{U}$ as the average over I of the contributions to the induced horizontal velocity from all N points, averaged as before over a cycle and evaluated for large t. Since this operation involves an x-integral of χ_{xy} we have

$$\overline{U} = f_0 \left\langle \int_0^t \frac{1}{N} \sum_{k=1}^N 2\pi \cos 2\pi\tau \left[\chi_y(L(k-0.5)/N - L - \sigma(t-\tau), \sin 2\pi t - \sin 2\pi\tau, t-\tau) \right.\right.$$

$$\left.\left. - \chi_y(L(k-0.5)/N - \sigma(t-\tau), \sin 2\pi t - \sin 2\pi\tau, t-\tau) \right] \mathrm{d}\tau \right\rangle. \tag{4.8}$$

The condition on f_0 is then

$$\pi = -\frac{f_0}{L} \left\langle \cos 2\pi t \int_0^t 2\pi \cos 2\pi\tau \left[2F(0, t, \tau) - F(-L, t, \tau) - F(L, t, \tau) \right] \mathrm{d}\tau \right\rangle, \tag{4.9}$$

where

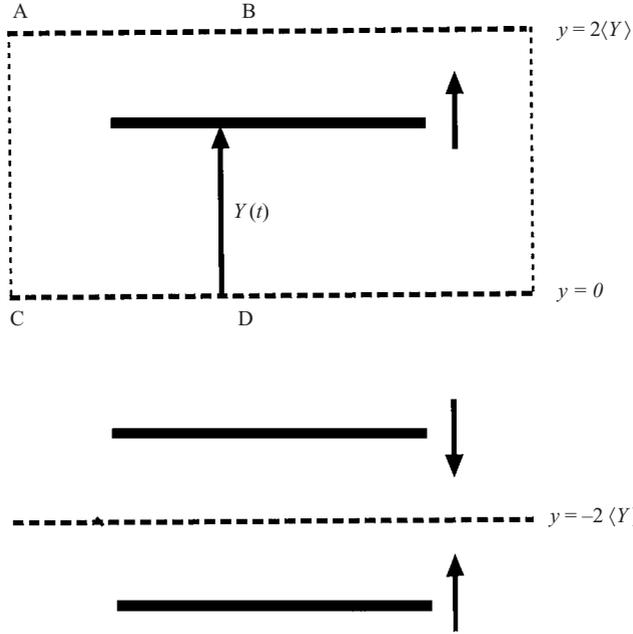$$F(x, t, \tau) = \chi(x - t + \tau, \sin 2\pi t - \sin 2\pi\tau, t - \tau). \tag{4.10}$$

FIGURE 8. The venetian blind model. The flow is horizontal. The oscillations are as shown by the arrows. The horizontal dotted lines are invariant streamlines of the flow field.

We have calculated three pairs (Re_ω, σ) where $\overline{U} = -1$, for $L = 1$, $\omega = 2\pi$, $k = 10$, and have included these points as the open circles in figure 5. Note that the general trend of the observational data is obeyed by this model. The calculations indicate $Re_{\omega c} = 33$.

5. The flapping venetian blind

We consider now a two-dimensional viscous flow model which allows an approximate calculation of the critical Reynolds number $Re_{\omega c}$ in a particular if somewhat artificial case. The 'flapper' is an infinite vertical periodic array of oscillating pairs of identical horizontal flat plates, which we shall call *slats*, all of chord unity, as shown in figure 8.

Each pair of slats oscillates in the vertical and in opposition, thus establishing reciprocal motion with a spatial period δ, equal to twice the average vertical spacing. The array might therefore be described best as an 'flapping venetian blind'. The model arose after first considering a single pair of plates, or a 'flapping biplane', the motion of the two wings against each other giving a crude model of the 'body slapping' seen in *Clione*. The advantage of periodic extension will be apparent below.

We suppose the array of wing pairs is the set

$$-1/2 \leqslant x \leqslant 1/2, \; y = 3k\langle Y(t)\rangle \pm Y(t), k = 0, \pm 1, \pm 2, \ldots, \\ |Y - \langle Y\rangle| < \langle Y\rangle, \tag{5.1}$$

where $\langle \cdot \rangle$ denotes the time average. Note that $\delta = 2\langle Y\rangle$.

We may assume that $Y(t)$ is periodic with period 1, and place a condition on its symmetry:

$$Y(t+1) = Y(t), \; Y(t+1/2) = \delta - Y(t). \tag{5.2}$$

Examples are $Y = \langle Y \rangle (1 + a \cos 2\pi t)$, $0 < a < 1$, or, in §5.1,

$$Y = \begin{cases} \delta & \text{if } 0 < t < 1/2, \\ 0 & \text{if } 1/2 < t < 1, \end{cases} \tag{5.3}$$

which we refer to as a square-wave cycle. With this symmetry the lines $y = \langle Y \rangle$ mod $2\langle Y \rangle = \delta/2$ mod δ are invariant streamlines of the flow, allowing us to effectively isolate a single slat within two invariant streamlines. We shall refer to the strips $0 < y < Y$ and $Y < y < \delta$ as *channels* associated with the slat having mean position $\delta/2$.

The dimensionless velocity at infinity will be σ. Thus the strip $0 < y < \delta$, bounded by horizontal streamlines, will carry a fixed fluid flux $\sigma\delta$. At each instant of time, this flux must be divided into a part $q(t)$ carried by the channel $0 < y < Y$, and a part $\sigma\delta - q(t)$ carried by the channel $Y < y < \delta$. We refer to these as (net) channel fluxes even though, as a result of the slat motion, the velocity and flux within a channel will vary with x.

We are interested in calculating the fluid motion which is generated when this system of planes is placed in a fixed uniform stream of viscous fluid. We show, under conditions to be described, that there is a unique value of Re_ω such that, at this value, the force per unit area exerted by the fluid upon the array, in the cross–flow plane, vanishes. Further, we shall find that, within the approximations we make, the force is zero at any free-stream velocity consistent with our assumptions, provided only that sufficient power is provided to maintain the oscillation of the blind.

In our model, δ is the aspect ratio of the rectangle formed by a pair of adjacent plates held in their mean positions. We make the basic assumption that $\delta \ll 1$. This will allow us to calculate the action of two adjacent slats on the fluid between them as if they were infinite planes. We shall examine two approaches to calculation of a critical value of Re_ω. We note first that if $\delta^2 Re_\omega \ll 1$ then at all instants of motion a Poiseuille channel flow is established over most of the channels between slats. If simultaneously $\delta Re_\omega \gg 1$, then within a distance of order δ of the ends of the slat, inviscid dynamics is obtained. Thus we can envisage an expansion for small $\delta^2 Re_\omega$ which is based upon perturbed Poiseuille flow with entry and exit conditions determined by an inviscid problem. We shall indicate in §5.2 how such an expansion proceeds. The main drawback of this approach is that a $Re_{\omega c}$ should satisfy $\delta^2 Re_{\omega c} = O(1)$, which means that the accuracy of a calculation of $Re_{\omega c}$ from a truncation of the expansion is questionable.

A second approach is to assume $\delta^2 Re_\omega \gg 1$, so that the flow throughout the channels may be taken as approximately inviscid. In §5.1 we consider this limit and show that it is consistent with the calculation of $Re_{\omega c}$ provided that the wing motion is instantaneous between its extreme positions (square-wave cycle). This motion will allow us to separate the flow analysis into a fast inertial phase where viscosity may be neglected, and a 'stasis' where the slats are held fixed and viscous diffusion of the momentum occurs. We shall find that $Re_{\omega c} = O(\delta^{-3})$ up to logarithmic terms.

A final limiting case worth consideration is where both δ and δRe_ω are small. Then Stokes flow prevails throughout, and we may make use of the principle of minimum viscous dissipation, see Batchelor (1967).† In this limit the dissipation is obtained by assuming Poiseuille flow over the entire length of a channel. This is easily minimized for given flux to obtain a flux through the channel $0 < y < Y$ given by

$$q(t) = \frac{\delta Y^3}{(\delta - Y)^3 + Y^3}. \tag{5.4}$$

† We thank J. B. Keller for suggesting this calculation.

The time-averaged drag per slat is then

$$\langle D \rangle = Re_\omega^{-1} \langle 6\delta Y [(\delta - Y)^3 + Y^3]^{-1} \rangle, \tag{5.5}$$

which is a quantity of order $Re_\omega^{-1}\delta^{-1}$.

5.1. *Analysis of the model with square-wave cycle*

Since we assume that $\delta \ll 1$ and that the 'blind' moves in a square-wave cycle, the flow within a slat pair can be treated neglecting entry and exit effects, that is, as if the channel were doubly infinite. We shall also neglect any effect of vorticity shed into the external fluid. This is reasonable because the motion of slat pairs is such that two vortices of opposite circulation are shed simultaneously. We further note that in this section the pressure is made dimensionless by division by density times $L^2\omega^2$.

5.1.1. *The inertial phase*

Suppose that at $t = 0$ two slats lie on top of each other at $y = \delta$ mod 2δ. We take the flow field in the region $|y| < \delta$ to be $U(y)$, some even function of y with $U(\pm\delta) = 0$. Since $\sigma\delta$ is the dimensionless mass flux through the blind, we must have

$$\int_0^\delta U(y)\,\mathrm{d}y = \delta\sigma. \tag{5.6}$$

Were U to be a Poiseuille channel flow, it would be given by $U = \frac{3}{2}\sigma(1 - (y/\delta)^2)$.

In the inertial phase slats at $y = \pm\delta$ abruptly move to $y = 0$. We thus refer to the terminal time of this phase as $t = 0+$. During this movement, the fluid between the slats is squeezed out, and the vorticity of the initial flow is advected inviscidly. Simultaneously the fluid fills the expanding channel bounded between the two slats initially at $y = \delta$. We will consider the fluid flow within the region $0 \leqslant y \leqslant \delta$, divided into the ejection channel $0 \leqslant y \leqslant Y$ and the injection channel $Y \leqslant y \leqslant \delta$. As the slat at δ moves to $y = 0$, a flow field $(-\dot{Y}x/Y, \dot{Y}y/Y)$ in the ejection channel advects the initial vorticity toward the line $y = 0$. Thus during the inertial phase the flow in the ejection channel is given by the following exact solution of Euler's equations:

$$u = -\frac{\dot{Y}x}{Y} + \frac{Y}{\delta}U\left(\frac{y\delta}{Y}\right) + u_1, \tag{5.7a}$$

$$v = \frac{\dot{Y}y}{Y}, \quad p = \frac{\ddot{Y}(x^2 - y^2)}{2Y} - \frac{\dot{Y}^2}{Y^2}x^2 + u_1\frac{\dot{Y}}{Y}x - \dot{u}_1 x \quad \text{(ejection)}. \tag{5.7b, c}$$

We have allowed here for a uniform flow $u_1(t)$, but will argue below that this term must vanish if the flow field is to represent correctly the effects of viscosity.

Similarly, in the injection channel $Y < y < \delta$ the filling flow has the form $(\dot{Y}x/(\delta - Y), -\dot{Y}y/(\delta - Y))$. As the slats separate we assume that a uniform flow $(u_2(t), 0), u_2(0) = 0$ is present to compensate for the flux no longer carried by the ejection region. The corresponding Euler flow will have the form

$$u = \frac{\dot{Y}x}{\delta - Y} + u_2(t), \tag{5.8a}$$

$$v = \frac{\dot{Y}(\delta - y)}{\delta - Y}, \tag{5.8b}$$

$$p = \frac{\ddot{Y}(x^2 - (y - Y)^2)}{2(\delta - Y)} - \frac{\dot{Y}^2}{(\delta - Y)^2}x^2 - u_2\frac{\dot{Y}}{\delta - Y}x - \dot{u}_2 x + p_2(t) \quad \text{(injection)}. \tag{5.8c}$$

During the collapse, the sum of the mass fluxes in the two sections must equal $\sigma\delta$:

$$\frac{Y^2}{\delta^2}\int_0^\delta U(s)\,\mathrm{d}s + u_1 Y + u_2(\delta - Y) = \sigma\delta. \tag{5.9}$$

Now we know that the integral on the left of (5.9) equals $\sigma\delta$. Thus

$$u_1 Y + u_2(\delta - Y) = \sigma\delta(1 - Y^2/\delta^2). \tag{5.10}$$

We now introduce a basic assumption which will in effect fix the circulation carried by a slat and determine a unique flow field. We assert now that $u_1(t) = 0$, that is, that a uniform flow cannot be established in the ejection region, although the corresponding flow u_2 can be established in the injection region. The idea is that, since vorticity within the flow is being expelled in the ejection region, the vorticity bound to the slat cannot be changed from the ejection side. The difference in the treatment of the uniform flow in the two regions is reminiscent of the difference, in a large tank of viscous fluid, between the injection of fluid at a jet, and its withdrawal at a sink. This condition, which we shall refer to here as the *outflow principle*, sets the flux in the ejection region at $q(t) = \sigma Y^2/\delta$, and that in the injection region as $\sigma\delta(1 - Y^2/\delta^2)$. If we focus on the region $0 < y < Y$, then we have that $q(t) = \sigma Y^2/\delta$ when $\dot{Y} < 0$ and $q(t) = \sigma(2Y - Y^2/\delta)$ when $\dot{Y} > 0$. Thus the outflow principle implies

$$q(t) = \sigma[Y + \mathrm{sgn}(\dot{Y})Y(1 - Y/\delta)]. \tag{5.11}$$

When compared with (5.4), we see that (5.11) introduces non-reciprocal fluid dynamics into a problem with reciprocal boundary motion, as a result of the asymmetric effects of viscosity at high local Reynolds numbers. Whenever (5.11) applies, we adopt movements such a the square-wave cycle, consisting of two abrupt motions, one up and one down, over a single cycle.

We proceeded to calculate, with assumption (5.11) on q, the x-force experienced during the inertial phase. Since our calculation at this point is for an inviscid fluid having no embedded vortex sheets, the only source of an x-force will be suction forces associated with vorticity singularities at the tips of the slat, and to compute these suction forces we must consider the flow in the vicinity of the entrance and exit. The only reasonable calculation that can be done is for irrotational flow, hence we replace the parallel flow $U(y, t)$ by a uniform flow with the same flux, $U(t) = \sigma Y/\delta$. The entire inertial flow is now irrotational. Of course for flat-plate slats the suction singularities replace the viscous stresses created by the vorticity shed from the slat tips in the real fluid.

We show in figure 9 a conformal map from the ζ-plane to the physical z-plane, the latter representing the left (entry) region of a channel, the slat being taken as semi-infinite. The mapping (see e.g. Churchill 1948) is given by

$$z = \frac{\delta}{\pi}[C - k\log(\zeta + 1) - (1 - k)\log(\zeta - 1)], \quad C = k\log\left(\frac{y}{1 - k}\right) + \log 2(1 - k) + \mathrm{i}\pi. \tag{5.12}$$

The point A in the ζ-plane is $(\xi_A = 2k - 1, 0)$. The parameter k is defined by $k\delta = Y$, and the argument of the logarithm is between $-\pi$ and $+\pi$.

The flow field for the problem we study is given by

$$u - \mathrm{i}v = \sigma - \frac{\dot{Y}}{\pi}\log\left(\frac{\zeta - 1}{\zeta + 1}\right) + \frac{2K}{\zeta - \xi_A}, \tag{5.13}$$
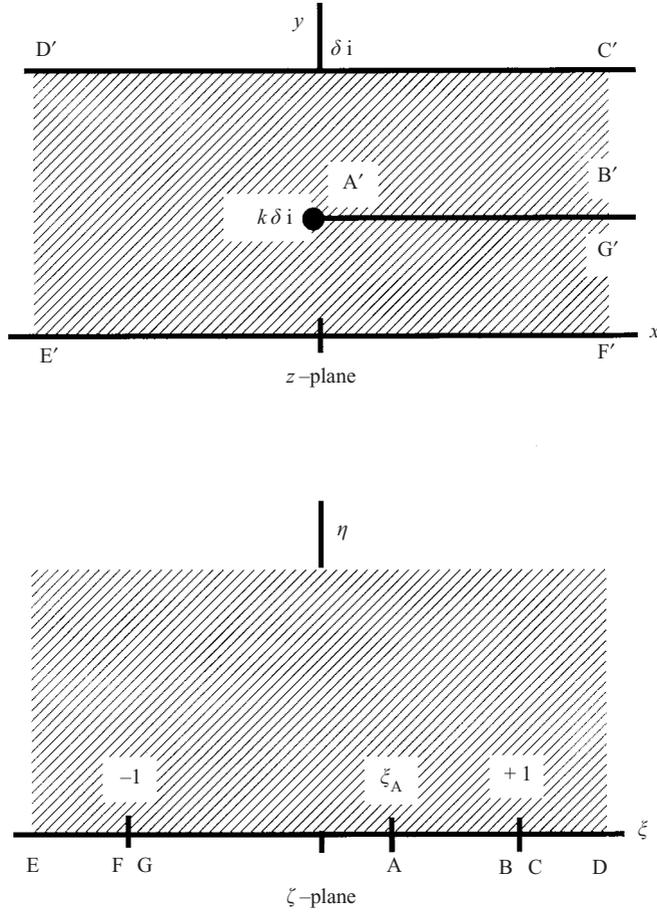
FIGURE 9. A conformal map of the entry region of a channel. The point A′ is the left edge of
the slat, and D′C′F′E′ outlines its channel. The domain is the upper half of the ζ-plane.

where K is a free constant. The term proportional to $\dot{Y}$ accounts for the motion of
the slat. The term proportional to K allows cancelling fluxes in the injection and
ejection channels, and essentially fixes the circulation of the slat.

To evaluate K it we consider the limit $\zeta \to -1$. Then $z \to \infty$ and

$$u - iv = \sigma + \frac{\dot{Y}}{\pi k}\left[k \log\left(\frac{k}{1-k}\right) + \log(1-k) - \pi z/\delta \right] - \frac{K}{k} + o(1). \qquad (5.14)$$

We thus require

$$\frac{\sigma Y}{\delta} = \sigma + \frac{\dot{Y}}{\pi k}\left[k \log\left(\frac{k}{1-k}\right) + \log(1-k) \right] - \frac{K}{k}, \qquad (5.15)$$

or, using $\delta k = Y$,

$$K = \frac{\sigma Y}{\delta}\left(1 - \frac{Y}{\delta}\right) + \frac{\dot{Y}}{\pi \delta}\left[Y \log\left(\frac{Y}{\delta - Y}\right) + \delta \log\left(\frac{\delta - Y}{\delta}\right) \right]. \qquad (5.16)$$

Consider now the singularity at the point A′ of the z-plane. If the vortex sheet
strength $\gamma(x)$ has a singularity of the form $2\alpha x^{-1/2}$ as $x \to 0+$ then there is a tip
suction force of magnitude $\pi\alpha^2$, see e.g. Durand (1963, p. 52). Near the point A

in the ζ-plane we have $u = \gamma/2 \approx 2K/(\zeta - \xi_A)$, and we find from (5.12) the local approximation

$$z - k\delta i = \frac{\delta}{8\pi k(1-k)}(\zeta - \xi_A)^2. \tag{5.17}$$

Thus

$$\pi \alpha^2 = \frac{K^2 \delta}{2k(1-k)}. \tag{5.18}$$

To consider the two ends of a slat, we may take the difference of the two values of K^2 obtained with $\pm\dot{Y}$ used in (5.16). The dominant expressions cancel and we are left with net suction force

$$
\begin{aligned}
S &= \frac{2\delta}{k(1-k)}\frac{\sigma Y}{\delta}\left(1 - \frac{Y}{\delta}\right)\frac{\dot{Y}}{\pi\delta}\left[Y\log\left(\frac{Y}{\delta-Y}\right) + \delta\log\left(\frac{\delta-Y}{\delta}\right)\right] \\
&= -\frac{2}{\pi}\sigma\dot{Y}\int_0^\delta Y\log Y + (\delta-Y)\log(\delta-Y)\,\mathrm{d}Y \\
&= \frac{\sigma\delta^2}{\pi}(1 - 2\log\delta).
\end{aligned} \tag{5.19}
$$

5.1.2. *The viscous phase*

We now consider the viscous phase. Since the inertial phase is taken as instantaneous, and we are describing one-half of a full flapping cycle, the viscous phase will last time $1/2$. We consider the region $0 < y < 2\delta$, bounded by two now stationary slats. During the inertial phase this region was filled by an inrush of fluid, which we take to be irrotational. At $t = 0+$ a flux of $2\sigma\delta$ is carried by this channel, so the initial velocity will be given by $u = u_0 = \sigma$. Subsequently we have $(u, v) = (u(y - \delta, t), 0)$ where $u(y, t)$ satisfies

$$u_t - \frac{1}{Re_\omega}u_{yy} = \Pi(t), \quad u(-\delta, t) = u(\delta, t) = 0, \quad \int_0^\delta u\,\mathrm{d}y = \sigma\delta. \tag{5.20}$$

The solution has the form

$$u = \frac{3}{2}\sigma\left[1 - \left(\frac{y}{\delta}\right)^2\right] + \sum_{n=1}^\infty a_n \exp(-\lambda_n^2 t/Re_\omega)\phi_n(y) \tag{5.21}$$

where $\phi_n = \cos(\lambda_n y) - \cos(\lambda_n\delta)$, $k_n = \delta\lambda_n$ are the positive roots of $\tan z = z$ arranged as an increasing sequence, and

$$a_n\int_0^\delta \phi_n^2\,\mathrm{d}y = \sigma\int_0^\delta \phi_n\left(1 - \frac{3}{2}\left[1 - \left(\frac{y}{\delta}\right)^2\right]\right)\,\mathrm{d}y. \tag{5.22}$$

One finds easily

$$a_n = 2\sigma/(k_n \sin k_n). \tag{5.23}$$

Twice the time integral from $t = 0+$ to $t = 1/2$ of the total viscous force exerted at $|x| < 1/2$, $y = \delta-$ is obtained from (5.21) as

$$D = \delta\sigma\left[\frac{3}{2\delta^2 Re_\omega} + 2\sum_{n=1}^\infty k_n^{-2}\left(1 - \exp(-k_n^2/(2\delta^2 Re_\omega))\right)\right]. \tag{5.24}$$

Note that (5.21) may be evaluated at $t = 1/2$ to get the function $U(y)$ which should actually begin the inertial phase.

δ	$Re_{\omega c}$
1	9.23
0.5	28.2
0.25	162

TABLE 1. Critical Reynolds number for various δ for the venetian blind flapper in square-wave mode.

5.1.3. *The critical Reynolds number*

The critical Reynolds number is obtained by equating the drag D to the suction force S, which yields the following equation for $\delta^2 Re_{\omega c}$:

$$\frac{\delta}{\pi}(1 - 2\log\delta) = \left[\frac{3}{2\delta^2 Re_{\omega c}} + 2\sum_{n=1}^{\infty} k_n^{-2}\left(1 - \exp\left[-k_n^2/(2\delta^2 Re_{\omega c})\right]\right)\right]. \quad (5.25)$$

We show some values of $Re_{\omega c}$ in Table 1.

The square-wave cycle has been analysed under several assumptions which disregard certain important real fluid effects. (i) Our replacement of $U(y)$, with $U(\delta-) = 0$, by a uniform flow tends to alter the flow near the tips in a manner which should probably decrease the suction force. We therefore surmise that the actual profile will lead to a reduction in $Re_{\omega c}$. (ii) It clear that in a real fluid and for a thin slat, the suction force computed here as an implied pressure force must be replaced by viscous stresses created at the walls by shed vorticity, see Batchelor (1967, p. 439), Wang (2000), and the discussion below. The venetian blind model in a real fluid is useful for understanding viscous thrust generation since the shed vorticity is firmly confined between the invariant streamlines of the channels. (iii) Some vorticity ejected upstream by the collapse of a channel can be drawn into the adjacent injection channels. The appropriate problem for the inertial phase would allow for a rotational inviscid flow. For simplicity we have neglected this effect and taken u_2 as a uniform flow.

5.2. *Formal expansion in $\delta^2 Re_\omega$*

As a second approach to computing a critical Reynolds number for the flapping venetian blind, we have investigated the formal expansion of the flow in powers of Re_ω, an expansion which can be written as an expansion in $\delta^2 Re_\omega$. If this latter parameter as well as δ is small, then to a first approximation the flow established within $|y| < Y$ is a Poiseuille channel flow with negligible entry and exit effects. We also must assume that $Y(t)$ is a smooth function of time, so the slat motion of the square-wave analysis is excluded. We have noted above that, since $\delta^2 Re_{\omega c}$ should be of order unity, we are faced with using a truncation of an expansion without control of the error. Nevertheless it is of interest to see what results are obtained since the approach is in a sense opposite to that used for the square-wave cycle.

This calculation is straightforward and is summarized in Appendix B. There arises again the issue of indeterminacy of the division of flux between injection and ejection regions. Let $q(t)$ be the mass flux in the channel $0 < y < Y$, so $q(t + 1/2)$ is the mass flux in the channel $Y < y < \delta$. Then the imposition of a fixed flux through the blind imposes the condition

$$\delta\sigma = q(t) + q(t + 1/2). \quad (5.26)$$

The two functions on the right are independent of each other and cannot be determined without some knowledge of the entry flow. We remark that momentum
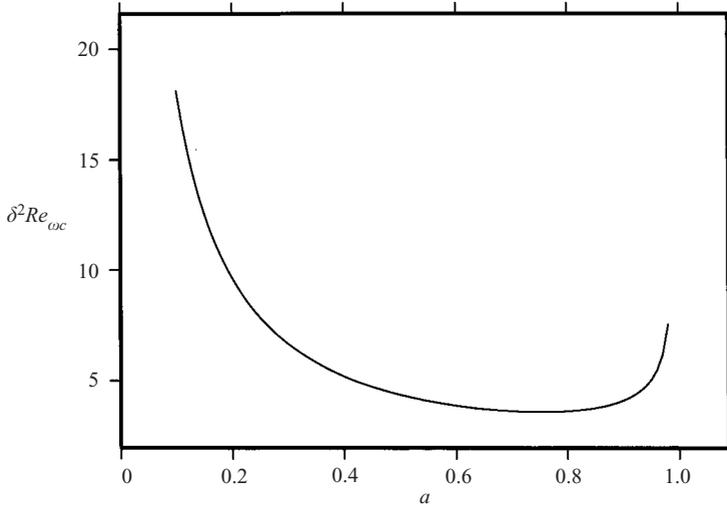
FIGURE 10. $\delta^2 Re_{\omega c}$ versus flapping amplitude a for the venetian blind in sinusoidal motion, as computed by expansion in $\delta^2 Re_\omega$ up to three terms.

conservation does not supply an additional relation, since the pressure downstream of the blind is a function of time, related directly to the instantaneous drag per unit area acting on the blind, see Appendix B. Momentum conservation through the entry serves only to determine the entry value of the static pressure.

To proceed further we must therefore assume $\delta Re_\omega \gg 1$ so that the outflow principle applies, with q given by (5.11). We then set $Y = \delta(1 + a\cos(2\pi t))/2$, and the following equation for the average drag $\langle D \rangle$ results:

$$\delta Re_\omega \sigma^{-1} \langle D \rangle = \frac{6}{\sqrt{1-a^2}} - \frac{18}{35} a\delta^2 Re_\omega - 0.1216 a^2 \delta^4 Re_\omega^2 + O\left(\delta^6 Re_\omega^3\right). \qquad (5.27)$$

Note that the term of order $\delta^2 Re_\omega$ arises here because of the non-reciprocal flux function. If we truncate the series at this order, we obtain the values of $Re_{\omega c}$ shown in figure 10.

For $a \approx 0.9$ the values of $Re_{\omega c}$ obtained here are close to the values for the square-wave cycle. They are larger than but not inconsistent with the observations of *Clione*, and the general shape of the curve suggests the importance of 'body slapping' for the reduction of $Re_{\omega c}$. If we take $Re_{\omega c} = 9/\delta^2$ with $\delta = 1$ to simulate body slapping as an 'image' slat, and take the body length to be twice the chord, then the $Re_{\omega c}$ based on wing chord would be about 33. Allowing for three-dimensional effects as well as the body drag, our number is well above the 5–20 range of *Clione*. We are using a severely truncated expansion, and a numerical simulation of the venetian blind model for various Re_ω and δ will be needed to pin down precisely $Re_{\omega c}(\delta)$ in this model.

6. A Navier–Stokes calculation of $Re_{\omega c}$ in two dimensions

Recent calculations of flapping flight in two dimensions by Jane Wang have utilized a high-accuracy Navier–Stokes code at Re of order 1000 (Wang 2000). The wing is of thin elliptical section. Wang has generously carried out for us some preliminary calculations with this code at lower Reynolds numbers for sinusoidal vertical motion with an amplitude of one-half the wing chord (total vertical wing excursion = wing

Re_f	Re_ω	Drag
16	32	−3.46
16	16	−0.066
16	8	1.01
32	32	−1.22
32	16	0.46
32	8	0.75
64	64	−6.62
64	32	0.02
64	16	0.41
64	8	0.5

TABLE 2. Drag calculations for Navier–Stokes flow past an flapping thin ellipse, amplitude of one-half chord.

chord). In these calculations, the reference length for the Reynolds numbers is the wing chord. The results are shown in table 2.

These values indicate $Re_{\omega c} \approx 15$, and that the bifurcation is supercritical. This number can be compared to the $Re_{\omega c}$ of 36 for the model Oseen model of a wing at an amplitude equal to the chord. Not surprisingly, the Oseen model considerably overestimates $Re_{\omega c}$ for flapping flight, probably more a result of the approximate force calculation than the Oseen linearization. On the other hand the value 15 agrees reasonably well with the venetian blind model in the square-wave cycle with $\delta = 1$, provided that slat interaction enhances thrust.

7. General considerations in three dimensions

We consider now the form taken by solutions of the Navier–Stokes equations for a general reciprocal flapper in three dimensions, given that a finite critical Reynolds number for flapping flight exists.

For simplicity we assume that the reciprocal motion is such that the centre of volume remains on the line $y = z = 0$, that it remains at $x = y = z = 0$ when placed there without an initial x-velocity and, once flapping flight takes place, is located at $(x, y, z) = (X(t), 0, 0)$ (we can accomplish this, for example, with a 'flapping biplane'). Let the time-dependent (dimensionless) flow velocity for the flapping body sitting at rest be $\boldsymbol{v}_0(x, y, z, t; Re_\omega)$, where $\boldsymbol{v}_0$ is periodic in time with period unity. We shall for convenience assume that Re_ω is changed by altering the viscosity.

Let $\sigma(t) = \mathrm{d}X/\mathrm{d}t$ denote the (small) instantaneous dimensionless velocity. We take $\delta Re_\omega \equiv Re_\omega - Re_{\omega c}$ and $\sigma(t)$ to be small, and assume that the latter changes slowly. Let $\sigma(0) = \sigma_0 > 0$ determine the initial releas velocity of the flapper. According to Newton's laws of motion, following release the total momentum of body and fluid, relative to coordinates at rest with respect to infinity, must remain constant and equal to the initial x-momentum of the body, $\sigma_0 m$ say, where m is the body mass:

$$M_b + M_f = \sigma_0 m = m\sigma(t) + M_f. \tag{7.1}$$

Thus

$$m\frac{\mathrm{d}\sigma}{\mathrm{d}t} = -\frac{\mathrm{d}M_f}{\mathrm{d}t} = F_f \tag{7.2}$$

where F_f is the force exerted on the body. In the region of the bifurcation we divide this force into two parts which can be regarded as thrust T and drag D,

$$m\frac{\mathrm{d}\sigma}{\mathrm{d}t} = T - D, \tag{7.3}$$

which shall now define and compute quasi-steadily and adiabatically by placing the flapper in a fixed wind and taking T and D as averages over one cycle of motion. We shall also assume the bifurcation is supercritical.

Let $\boldsymbol{v}_c(x, y, z, t)$ be the velocity perturbation caused by placing the flapper, operating at critical, in the wind. The problem satisfied by $\boldsymbol{v}_c$ is then

$$Re_{\omega c}\left[\frac{\partial \boldsymbol{v}_c}{\partial t} + \sigma\frac{\partial \boldsymbol{v}_c}{\partial x} + \boldsymbol{v}_c \cdot \nabla \boldsymbol{v}_c\right] + \nabla p_c - \nabla^2 \boldsymbol{v}_c = 0, \tag{7.4a}$$

$$\boldsymbol{v}_c|_{B(t)} = -\sigma\boldsymbol{i}, \quad \boldsymbol{v}_c|_\infty = 0. \tag{7.4b}$$

Here $B(t)$ denotes the body surface. Since the bifurcation is supercritical, the average force experienced when operating at critical is drag, so $\boldsymbol{v}_c$ determines the $D(\sigma)$ in (7.3). Its expansion for small σ contains no term linear in σ, so

$$D = o(\sigma), \quad \sigma \to 0. \tag{7.5}$$

Now let the solution for $Re_\omega = Re_{\omega c} + \delta Re_\omega$ be $\boldsymbol{v} = \boldsymbol{v}_c + \delta\boldsymbol{v}$. Now $\delta\boldsymbol{v}$ satisfies an analogous problem with null conditions on the same body surface $B(t)$. The linear equation satisfied by a small $\delta\boldsymbol{v}$ is

$$Re_{\omega c}\left[\frac{\partial \delta\boldsymbol{v}}{\partial t} + \sigma\frac{\partial \delta\boldsymbol{v}}{\partial x} + \delta\boldsymbol{v} \cdot \nabla \boldsymbol{v}_c + \boldsymbol{v}_c \cdot \nabla \delta\boldsymbol{v}\right] + \nabla \delta p - \nabla^2 \delta\boldsymbol{v} = -\delta Re_\omega \boldsymbol{v}_c \cdot \nabla \boldsymbol{v}_c. \tag{7.6}$$

Thus $\delta\boldsymbol{v} = O(\delta Re_\omega)$ and the corresponding force will have a term linear in σ, which is the thrust developed above the critical value of Re_ω. This determines T in (7.3). We then obtain an equation of the form

$$m\frac{\mathrm{d}\sigma}{\mathrm{d}t} = c_1(Re_\omega - Re_{\omega c})\sigma - D(\sigma), \tag{7.7}$$

which is consistent with what we see in figure 5 if $D(\sigma) = O(\sigma^2)$. The leading term of D should depend on body shape, and in general we expect $D = O(\sigma^2)$, but we have not ruled out that the leading term could be $O(\sigma^3)$ in some cases. It is not clear from figure 7 what asymptotic behaviour is obtained for the oscillating Oseenlet, although the higher power is suggested. We emphasize that the nonlinear term in (7.4a) is needed to reach equilibrium. This is the reason for our claim that the bifurcation to reciprocal flapping flight is necessarily accompanied by departure from the Stokesian realm of locomotion.

These general arguments have their counterpart in the venetian blind model, but since the problem is linear in σ (see Appendix B), the only nonlinearity can come from a modification of the model by the addition of a passive element producing drag, see figure 11. Then if $Re_\omega > Re_{\omega c}$ we have $\langle D \rangle = D_B$, where D_B is the dimensionless drag of the attached body. Once supercritical,

$$D_B = C\frac{Re_f}{Re_\omega^2}(Re_\omega - Re_{\omega c}), \tag{7.8}$$

where C is a positive constant. In our dimensionless formulation, in the Stokesian realm, body drag would be $K\nu L U_f$ for some positive constant K or in dimensionless
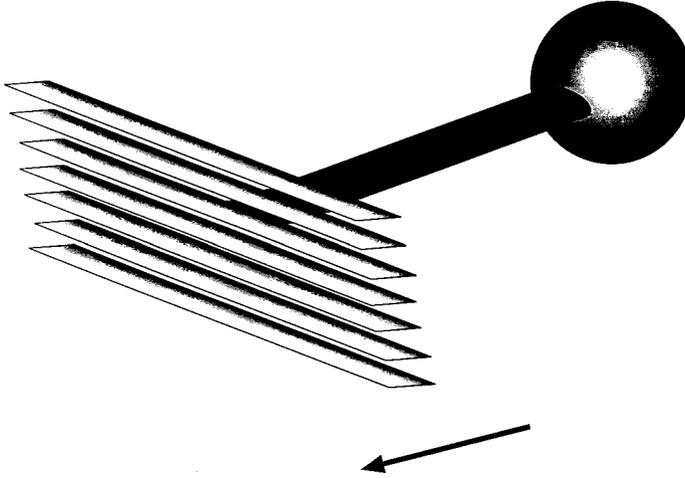
FIGURE 11. Finite venetian blind locomotor dragging a body.

form $K Re_f / Re_\omega^2$ per unit area of blind. Thus $K = C(Re_\omega - Re_{\omega c})$ and Re_f remains undetermined.

We must then modify the drag law by a nonlinear correction,

$$D_B = K Re_f / Re_\omega^2 (1 + \alpha Re_f), \quad \alpha > 0, \tag{7.9}$$

corresponding to a deviation from Stokes' drag determined by the quadratic term in the flow velocity. Now the supercritical speed U_f is given by

$$Re_f = \frac{1}{\alpha} \frac{C}{K}(Re_\omega - \overline{Re_{\omega c}}), \quad \overline{Re_{\omega c}} = Re_{\omega c} + \frac{K}{C}. \tag{7.10}$$

Thus we are led again to a bifurcation diagram which may be compared with figure 5.

8. Discussion

The fluid dynamics describing the relative motion of 'solid' material and fluid divides roughly into two categories. On the one hand, the fluid can be transported though the solid, as in Poiseuille flow through a pipe. On the other hand, the body may move through the fluid, as in the locomotion of fish. These complementary problems share a number of common features, including an appropriate division into Stokesian and Eulerian realms (Lighthill 1975). The analogue of the non-reciprocal, Stokesian swimmer is the peristaltic pump, see Jaffrin & Shapiro (1971) and Childress (1981b). In peristalsis, waves of contraction move down a flexible pipe and are able to transport fluid at a fixed rate determined by the frequency of the pumping cycle. More recently, investigations of 'valveless pumping' at high Reynolds numbers have demonstrated similar properties of transport in the Eulerian realm, using reciprocal motions of the pipe wall (Jung 1999; Jung & Peskin 2001).

The models considered in the present paper involve elements of both categories of problems. Oscillatory channel flow such as we have applied in the venetian blind model can be usefully applied to study peristalsis, see Jaffrin & Shapiro (1971). In a sense the venetian blind model is an attempt to introduce the simpler fluid transport modelling into the more difficult problem of locomotion.

If the study is restricted to the Eulerian realm, symmetry-breaking bifurcations may occur in these problems. Valveless pumping due to deformations of a tube which

are symmetric with respect to a plane perpendicular to the tube axis can pump fluid in either direction, depending upon the initial conditions. In forward flapping flight, the classical linear inviscid analysis of a flapping plate of chord L, in sinusoidal motion, leads to a drag $-\rho\omega^2 L^3 f(|\sigma|)$, where $f(0) > 0$, $f(x) \sim C/x$, $x \to \infty$, see Durand (1963). Thus a thrust force on the plate, opposite to the flow direction, is realized for flow in either direction. Symmetry-breaking bifurcations may occur for general flapping bodies whose movements are symmetric with respect to some co-moving plane, for motion perpendicular to the plane. This point has been emphasized recently in the interesting context of take-off of a butterfly from a horizontal plane by Imai & Yanagita (2001). In that problem motion is vertical and the flapping is reciprocal and symmetric with respect to a plane through the hinge point.

In these Eulerian problems the bifurcation occurs because of the advection of vorticity relative to the body, and so is related to the bifurcation we study here. On the other hand the bifurcation with respect to Re_ω involves a competition between advection and diffusion, and there is no special assumption regarding the fore–aft symmetry of the body or the motion.

The variation with Reynolds number of the thrust achieved in flapping flight is of some theoretical interest because of the role of viscosity in the process, even when the Reynolds number is arbitrarily large. According to classical inviscid theories of lift (and thrust) developed by an airfoil (see e.g. Batchelor 1967, ch. 6 and Lighthill 1975), the leading and trailing edges of the foil are assigned distinctly different roles in determining circulation. In particular the Kutta–Joukowsky condition is imposed at a sharp trailing edge, to ensure that the inviscid solution has no strong singularity there. This leads to a smooth flow off the trailing edge, approximating what is observed. This condition on the inviscid theory is intended to reflect the action of viscous boundary layers, which in fact develop downstream and introduce a fore–aft asymmetry into the problem.

For edges which are not sharp, and for Reynolds numbers which are not extremely large, there is no satisfactory theory to replace the classical Kutta–Joukowsky condition, and as $Re \to 0$ the distinction between fore and aft edges disappears. In the case of flapping flight, for example the up-and-down movement in two dimensions of a flat plate aligned parallel to the horizontal free stream, vorticity is generated and shed from both edges. The vorticity is shed predominately from the downstream edge at large Re, and is diffused equally from both edges at small Re. Since the configuration of shed vorticity is ultimately responsible for the instantaneous forces experienced by the foil, the evolution of this vorticity field must ultimately account for a transitional Reynolds number of the kind we study here. Various simple explanations may be devised for recovery of thrust in particular situations. For example, a flapping flat plate produces on the upstroke a symmetric pair of shed vortices in the absence of a wind. A wind carries these vortices downstream, allowing the upstream vortex to create a viscous thrust on the lower surface before another pair of vortices of opposite sign is created on the downstroke. A great variety of mechanisms is possible from more elaborate movements.

Thus the linear instability associated with bifurcation to flapping flight must ultimately be understood in terms of the infinitesimal displacements of the vorticity field created by the flapping wings, when the body is moved slightly through the fluid. The saturation at constant speed of locomotion must similarly be accounted for by large displacements of the shed vorticity over a flapping cycle.

The empirical observations and theoretical calculations described in this paper demonstrate that larval stages of *Clione antarctica* experience a critical value of

Re based upon body length in the range of 5–20. Results of the venetian blind model support the conjecture that 'body slapping' contributes substantially to the locomotion of *Clione*. Wing–body interactions are often neglected in the study of flapping flight, but are reminiscent of the contralateral wing effects in the 'clap and fling' used by some insects at higher Reynolds numbers, see Lighthill (1975) and Dudley (2000). Numerical evidence suggests that an isolated flat-plate wing will have a critical value of *Re* in the range of 5–20, based upon chord length, but clearly dependent upon oscillatory amplitude and frequency. Reynolds numbers of the wing chord for much larger *Clione* with both absolutely and relatively larger wings typically exceed those of the ascending body by a factor of 2–4 (unpublished data), but the possible role of non-reciprocal wing kinematics, dorsoventral morphological asymmetries, ciliary contributions, and body interactions must be kept in mind in such comparisons. Nonetheless, these results suggest that morphological transformation of the locomotor apparatus is mandated for all taxa, vertebrate or invertebrate, that ontogenetically transit this range of Reynolds numbers. Metamorphosis, in particular, might be expected to occur within this range in many taxa. For *Clione* specifically, the facultative use by individuals of wings to effect locomotion nicely exemplifies this functional dichotomy imposed by fluid mechanical constraints.

For flapping movements of a more general kind, not strictly reciprocal, the crossover from cilia to flapping may depend upon the relative power requirements and efficiencies of the two modes. We can estimate that in the lower end of the intermediate Reynolds number range 5–20, the force exerted by a wing is $\sim \nu \omega L^2$ and so the power required for flapping is $\sim \nu \omega^2 L^3$. On the other hand the drag of the organism is $\sim \nu U L$, and the work done by the drag force is $\sim \nu U^2 L$ so an efficiency is given by the ratio of the latter to the former, $\sim \sigma^2$. The rapid rise of σ as Reynolds number falls below the intermediate range, shown in figure 4, suggests that flapping can be considered ineffective below $Re \approx 5$.

In summary, we have attempted in this paper to explain observations of bimodal swimming of a pteropod mollusc in terms of the existence of a critical Reynolds number for flapping flight. Below this critical number, the flapping mode is ineffective and mechanisms appropriate to the Stokesian realm, such as the ciliary propulsion of *Clione antarctica*, must prevail. Above the critical Reynolds number, locomotion by flapping is realized, given a suitable initial 'push'. The equilibrium velocity in flapping flight is then determined by nonlinear processes. The resulting fluid dynamics should then move abruptly toward the high Reynolds number or Eulerian realm.

Although the transition from ciliary to flapping locomotion in *Clione antarctica* is not especially dramatic at the Reynolds numbers of our observations, the implications of the bifurcation to reciprocal flapping flight may deserve further study in the evolutionary context of natural locomotion. We conjecture that the biological record generally might reflect the bifurcation discussed here, if an (Re_ω, Re_f) plot obtained for many species yields values in the range $1 < Re_\omega < 100$. Reciprocal flapping brings into play the advection of vorticity, as an alternative to its diffusion, leading ultimately to the larger speeds and body sizes we associate with flying and swimming in nature.

Appendix A. A classical drag formula by unsteady analysis

In this Appendix we take the reference velocity to be the cylinder velocity U, so that $\sigma = 1$ and $\epsilon = Re^{-1}$ in (4.1).

We compute, for small r and large t,

$$I(x, y, t) \equiv \int_0^t \chi_{yy}(x - t + \tau, y, t - \tau). \tag{A 1}$$

But $\chi_{xx} + \chi_{yy} = \exp[-r^2/(4\epsilon t)]/(4\pi\epsilon t)$ and

$$\chi_{xx}(x - t + \tau, y, t - \tau) = \frac{\partial}{\partial \tau}\chi_x(x - t + \tau, y, t - \tau) + \chi_{xt}(x - t + \tau, t, t - \tau). \tag{A 2}$$

Thus

$$I = \chi_x(x - t, y, t) - \chi_x(x, y, 0) + \int_0^t \frac{1}{4\pi\epsilon(t - \tau)} \exp\left[-\frac{(x - t + \tau)^2 + y^2}{4\epsilon(t - \tau)}\right] d\tau$$

$$+ \int_0^t \frac{x - t + \tau}{8\pi\epsilon(t - \tau)^2} \exp\left[-\frac{(x - t + \tau)^2 + y^2}{4\epsilon(t - \tau)}\right] d\tau.$$

$$= \chi_x(x - t, y, t) - \chi_x(x, y, 0) + \int_0^t \frac{1}{8\pi\epsilon(t - \tau)} \exp\left[-\frac{(x - t + \tau)^2 + y^2}{4\epsilon(t - \tau)}\right] d\tau$$

$$+ \int_0^t \frac{x}{8\pi\epsilon(t - \tau)^2} \exp\left[-\frac{(x - t + \tau)^2 + y^2}{4\epsilon(t - \tau)}\right] d\tau. \tag{A 3}$$

Now $\chi_x(x - t, y, t)$ vanishes as $t \to \infty$ and $-\chi_x(x, y, 0) = -x/(2\pi r^2)$. Letting $r^2 = a^2 \ll 1$ and averaging the term in x^2 over the circle $r = a$, an operation we indicate by AVE (so as to apply Faxén's law), we obtain

$$AVE \int_0^t \frac{x}{8\pi\epsilon(t - \tau)^2} \exp\left[-\frac{(x - t + \tau)^2 + y^2}{4\epsilon(t - \tau)}\right] d\tau \sim \frac{x}{2\pi r^2} + \frac{1}{8\pi\epsilon} + o(1) \tag{A 4}$$

as $a \to 0$ and $t \to \infty$. Also

$$\int_0^t \frac{1}{8\pi\epsilon(t - \tau)} \exp\left[-\frac{(x - t + \tau)^2 + y^2}{4\epsilon(t - \tau)}\right] d\tau \sim -\frac{1}{4\pi\epsilon}\left(\gamma + \log\left(\frac{a}{4\epsilon}\right)\right) + o(1). \tag{A 5}$$

We note that we can get these results by dividing the integral

$$I(a) \equiv \int_0^\infty \frac{1}{8\pi\epsilon u} \exp\left(-\frac{1}{4\epsilon}[u + a^2/u]\right) du \tag{A 6}$$

into integrals from 0 to a and a to ∞. This leads to two equal integrals whose value may be compared with an exponential integral. This comparison uses

$$\int_1^\infty \left[\frac{1}{\sqrt{z^2 - 1}} - \frac{1}{z}\right] dz = \ln 2. \tag{A 7}$$

Finally, we can use $\frac{1}{2}a \, dI/da$ to compute the other integral appearing once the average is taken.

Thus we get

$$AVE(u) \sim \frac{1}{4\pi\epsilon}\left[\frac{1}{2} - \gamma - \log\left(\frac{a}{4\epsilon}\right)\right] + o(a), \tag{A 8}$$

which is the classical result giving, for a circular cylinder for $a \ll \epsilon$,

$$C_D \approx \frac{4\pi\epsilon}{\frac{1}{2} - \gamma - \log(a/4\epsilon)}, \tag{A 9}$$

see Lamb (1945).

Appendix B. The channel expansion

Since the condition $\delta^2 Re_\omega \ll 1$ allows a treatment as viscous channel flow, we may assume that in the domain $|y| \leqslant Y(t)$ the velocity will have the form

$$u = [xf(y, t, Re_\omega) + g(y, t, Re_\omega)], \quad v = h(y, t, Re_\omega), \tag{B 1a}$$

$$p = \tfrac{1}{2}x^2\Gamma(t) - \Pi x + P(y, t, Re_\omega), \tag{B 1b}$$

where $\Pi(t)$ is a function of time to be determined after the channel flow has been obtained. We require that f, g be even in y, that h be odd in y, and that

$$f(Y, t) = g(Y, t) = 0, \quad h(Y, t) = \dot{Y} \equiv \frac{\mathrm{d}Y}{\mathrm{d}t}. \tag{B 2}$$

The equations to be satisfied by g, h are then seen to be

$$g_{yy} + \Pi = Re_\omega[g_t - h_y g + h g_y], \quad h_{yyy} + \Gamma = -Re_\omega[h_{ty} - h_y^2 + h h_{yy}], \tag{B 3}$$

with

$$f = -h_y, \quad Re_\omega[h_t + h h_y] + P_y - h_{yy} = 0, \tag{B 4}$$

the latter being equations determining f and $P(y, t)$ up to an unimportant function of time. Note that the pressure term quadratic in x, together with f, h, are associated with the symmetric 'squeeze flow' due to the oscillation of the walls, g and Π with an oscillating unidirectional oscillatory Poiseuille flow and its interaction with the squeeze flow.

We introduce $\eta = y/Y(t)$ as a new independent variable, together with the new functions

$$F(\eta, t) = f(y, t), \quad G(\eta, t) = g(y, t), \quad H(\eta, t) = h(y, t). \tag{B 5}$$

The equations for G, H are then

$$\frac{1}{Y^2}G_{\eta\eta} + \Pi = Re_\omega\left[G_t - \frac{\dot{Y}}{Y}\eta G_\eta - \frac{1}{Y}(G H_\eta - H G_\eta)\right], \tag{B 6a}$$

$$Y^{-3}H_{\eta\eta\eta} + \Gamma = Re_\omega\left[\frac{1}{Y}H_{\eta t} - \frac{\dot{Y}}{Y^2}(H_\eta + \eta H_{\eta\eta}) - \frac{1}{Y^2}(H_\eta^2 - H H_{\eta\eta})\right]. \tag{B 6b}$$

The boundary conditions at $\eta = 0, 1$ to be imposed on G, H are then

$$G_\eta(0) = H(0) = H_{\eta\eta}(0) = G(1) = H_\eta(1) = 0, \quad H(1) = \dot{Y}. \tag{B 7}$$

These six conditions uniquely determine G, H, Γ.

The force on a slat is given by

$$D(t) = \frac{1}{Re_\omega}\left[-\frac{1}{Y(t)}G_\eta(1, t) + \frac{1}{Y(t+1/2)}G_\eta(-1, t+1/2)\right], \tag{B 8}$$

there being no contribution from F since the component of u is odd in x.

We seek to solve (B 6) subject to (B 7) as a power series:

$$(G, H, \Gamma) = \sum_{k=0}^{\infty} Re_\omega^k (G_k, H_k, \Gamma_k)(y, t). \tag{B 9}$$

After inserting the power series (B 9) into (B 6), we see from the boundary conditions (B 7) that

$$\Gamma_0 = 3\dot{Y}Y^{-3}, \quad G_0 = \tfrac{1}{2}\Pi Y^2(1-\eta^2), \quad H_0 = \tfrac{3}{2}\dot{Y}(\eta - \eta^3/3). \tag{B 10}$$

The first-order terms, of order Re_ω, satisfy

$$(G_1)_{\eta\eta} = \tfrac{1}{2}\dot{\Pi}Y^4(1-\eta^2) + \tfrac{1}{4}\Pi Y^3\dot{Y}(1-\eta^4), \tag{B 11a}$$

$$(H_1)_{\eta\eta\eta} + Y^3\Gamma_1 = \tfrac{3}{2}Y^2\ddot{Y}(1-\eta^2) - \tfrac{3}{4}Y\dot{Y}^2(5 - 6\eta^2 + \eta^4). \tag{B 11b}$$

Using the boundary conditions we then obtain

$$G_1 = \tfrac{1}{24}\dot{\Pi}Y^4(6\eta^2 - \eta^4 - 5) + \tfrac{1}{8}\Pi\dot{Y}Y^3\left(\eta^2 - \tfrac{1}{15}\eta^6 - \tfrac{14}{15}\right), \tag{B 12a}$$

$$H_1 = -\tfrac{1}{6}Y^3\Gamma_1\eta^3 + \tfrac{3}{2}Y^2\ddot{Y}\left(\tfrac{1}{6}\eta^3 - \tfrac{1}{60}\eta^5\right) - \tfrac{3}{4}Y\dot{Y}^2\left(\tfrac{5}{6}\eta^3 - \tfrac{1}{10}\eta^5 + \tfrac{1}{210}\eta^7\right) + C_1\eta, \tag{B 12b}$$

$$\Gamma_1 = \frac{6}{5}\frac{Y^2\ddot{Y}}{Y^3} - \frac{102}{35}\frac{Y\dot{Y}^2}{Y^3}, \quad C_1 = -\frac{1}{40}Y^2\ddot{Y} + \frac{19}{280}Y\dot{Y}^2. \tag{B 12c}$$

The terms of second order satisfy

$$(G_2)_{\eta\eta} \equiv g_2 = Y^2(G_1)_t - Y\dot{Y}\eta(G_1)_\eta - Y[G_0(H_1)_\eta$$
$$+ G_1(H_0)_\eta - H_0(G_1)_\eta - H_1(G_0)_\eta], \tag{B 13a}$$

$$(H_2)_{\eta\eta\eta} + Y^3\Gamma_1 \equiv h_2 = Y^2(H_1)_{\eta t} - Y\dot{Y}[(H_1)_\eta + \eta(H_1)_{\eta\eta}]$$
$$- Y[2(H_0)_\eta(H_1)_\eta - H_0(H_1)_{\eta\eta} - H_1(H_0)_{\eta\eta}]. \tag{B 13b}$$

With the help of the Symbolic Math Toolbox of MATLAB, we find

$$g_2 = \frac{1}{280}\dot{Y}^2\Pi Y^4\eta^8 + \left(\left(\frac{-11}{240}\ddot{Y}\Pi + \frac{1}{80}\dot{Y}\dot{\Pi}\right)Y^5 + \frac{7}{80}\dot{Y}^2\Pi Y^4\right)\eta^6 + \left(-\frac{1}{24}\ddot{\Pi}Y^6\right.$$
$$+ \left(\frac{7}{80}\ddot{Y}\Pi - \frac{1}{16}\dot{Y}\dot{\Pi}\right)Y^5 - \frac{109}{560}\dot{Y}^2\Pi Y^4\right)\eta^4 + \left(\frac{1}{4}\ddot{\Pi}Y^6 + \left(\frac{1}{16}\ddot{Y}\Pi + \frac{11}{16}\dot{Y}\dot{\Pi}\right)Y^5\right.$$
$$\left.+ \frac{5}{16}\dot{Y}^2\Pi Y^4\right)\eta^2 - \frac{5}{24}\ddot{\Pi}Y^6 + \left(-\frac{5}{48}\ddot{Y}\Pi - \frac{51}{80}\dot{Y}\dot{\Pi}\right)Y^5 - \frac{117}{560}\dot{Y}^2\Pi Y^4. \tag{B 14}$$

The term G_2 is then given by

$$G_2 = \frac{1}{25200}\dot{Y}^2\Pi Y^4\eta^{10} + \left(\left(\frac{1}{4480}\dot{Y}\dot{\Pi} - \frac{11}{13440}\ddot{Y}\Pi\right)Y^5 + \frac{1}{640}\dot{Y}^2\Pi Y^4\right)\eta^8$$
$$+ \left(-\frac{1}{720}\ddot{\Pi}Y^6 - \frac{109}{16800}\dot{Y}^2\Pi Y^4 + \left(\frac{7}{2400}\ddot{Y}\Pi - \frac{1}{480}\dot{Y}\dot{\Pi}\right)Y^5\right)\eta^6$$
$$+ \left(\frac{5}{192}\dot{Y}^2\Pi Y^4 + \frac{1}{48}\ddot{\Pi}Y^6 + \left(\frac{11}{192}\dot{Y}\dot{\Pi} + \frac{1}{192}\ddot{Y}\Pi\right)Y^5\right)\eta^4$$
$$+ \left(-\frac{117}{1120}\dot{Y}^2\Pi Y^4 - \frac{5}{48}\ddot{\Pi}Y^6 + \left(-\frac{51}{160}\dot{Y}\dot{\Pi} - \frac{5}{96}\ddot{Y}\Pi\right)Y^5\right)\eta^2$$
$$+ \frac{61}{720}\ddot{\Pi}Y^6 + \frac{3359}{40320}\dot{Y}^2\Pi Y^4 + \left(\frac{1003}{22400}\ddot{Y}\Pi + \frac{3539}{13440}\dot{Y}\dot{\Pi}\right)Y^5. \tag{B 15}$$

For H we similarly find

$$h_2 = \frac{3}{280}\dot{Y}^3 Y^2 \eta^8 + \left(\left(-\frac{7}{20}\dot{Y}\ddot{Y} + \frac{1}{4}\dot{Y}^2\right)Y^3 + \frac{3}{20}\dot{Y}^3 Y^2\right)\eta^6$$

$$+ \left(-\frac{1}{40}Y^{(3)}Y^4 + \left(-\frac{9}{10}\dot{Y}^2 + \frac{31}{40}\dot{Y}\ddot{Y} - \dot{Y}\left(-\frac{1}{8}\ddot{Y} - \frac{1}{2}\dot{Y}\right)\right)Y^3 - \frac{153}{140}\dot{Y}^3 Y^2\right)\eta^4$$

$$+ \left(\frac{3}{20}Y^{(3)}Y^4 + \left(-\frac{69}{70}\dot{Y}\ddot{Y} + \frac{9}{20}\dot{Y}^2 - \dot{Y}\left(\frac{3}{20}\ddot{Y} + \frac{3}{10}\dot{Y}\right)\right)Y^3 + \frac{117}{140}\dot{Y}^3 Y^2\right)\eta^2$$

$$- \frac{1}{4}Y^{(3)}Y^4 + \frac{13}{70}\dot{Y}\ddot{Y}Y^3 - \frac{57}{280}\dot{Y}^3 Y^2, \tag{B 16}$$

$$H_2 = \frac{1}{92400}\dot{Y}^3 Y^2 \eta^{11} + \left(\left(-\frac{1}{1440}\dot{Y}\ddot{Y} + \frac{1}{2016}\dot{Y}^2\right)Y^3 + \frac{1}{3360}\dot{Y}^3 Y^2\right)\eta^9$$

$$+ \left(-\frac{1}{8400}Y^{(3)}Y^4 - \frac{51}{9800}\dot{Y}^3 Y^2 + \left(-\dot{Y}\left(-\frac{1}{420}\dot{Y} - \frac{1}{1680}\ddot{Y}\right)\right.\right.$$

$$\left.\left. + \frac{31}{8400}\dot{Y}\ddot{Y} - \frac{3}{700}\dot{Y}^2\right)Y^3\right)\eta^7 + \left(\frac{39}{2800}\dot{Y}^3 Y^2 + \frac{1}{400}Y^{(3)}Y^4 + \left(-\frac{23}{1400}\dot{Y}\ddot{Y} + \frac{3}{400}\dot{Y}^2\right.\right.$$

$$\left.\left. - \dot{Y}\left(\frac{1}{400}\ddot{Y} + \frac{1}{200}\dot{Y}\right)\right)Y^3\right)\eta^5 + \left(-\frac{349}{25872}\dot{Y}^3 Y^2 - \frac{13}{2800}Y^{(3)}Y^4\right.$$

$$\left. + \left(\frac{181}{6300}\dot{Y}\ddot{Y} - \frac{13}{3150}\dot{Y}^2 + \frac{1}{2}\dot{Y}\left(\frac{1}{120}\dot{Y} - \frac{1}{240}\ddot{Y}\right) - \frac{1}{2}\dot{Y}\left(\frac{11}{4200}\dot{Y} - \frac{19}{8400}\ddot{Y}\right)\right)Y^3\right)\eta^3$$

$$+ \left(\frac{19}{8400}Y^{(3)}Y^4 + \frac{1153}{258720}\dot{Y}^3 Y^2 + \left(-\frac{187}{16800}\dot{Y}\ddot{Y} + \frac{1}{2400}\dot{Y}^2 - \frac{1}{2}\dot{Y}\left(\frac{1}{120}\dot{Y} - \frac{1}{240}\ddot{Y}\right)\right.\right.$$

$$\left.\left. + \frac{3}{2}\dot{Y}\left(\frac{11}{4200}\dot{Y} - \frac{19}{8400}\ddot{Y}\right)\right)Y^3\right)\eta. \tag{B 17}$$

Recalling the mass balance $\delta\sigma = q(t) + q(t + 1/2)$, we have

$$q(t) = q_0 + Re_\omega q_1 + Re_\omega^2 q_2 + \dots. \tag{B 18}$$

We obtain from the results given above,

$$q_0 = \dot{Y} + \tfrac{1}{3}Y^3 \Pi, \tag{B 19a}$$

$$q_1 = -\frac{2}{15}\dot{\Pi}Y^5 - \frac{8}{105}\Pi\dot{Y}Y^4, \tag{B 19b}$$

$$q_2 = \frac{17}{315}\ddot{\Pi}Y^7 + \left(\frac{53}{315}\dot{Y}\dot{\Pi} + \frac{136}{4725}\ddot{Y}\Pi\right)Y^6 + \frac{6421}{121275}\dot{Y}^2 \Pi Y^5 \tag{B 19c}$$

Note that the term $\dot{Y}$ in (B 19a) will not contribute to $q(t)$ since $\dot{Y}(t + 1/2) = -\dot{Y}(t)$. This is a crucial aspect of mass balance, which results from the mass flux ejected from a squeeze flow in one channel re-entering an adjacent, expanding channel.

The conservation of x-momentum can be similarly considered. Momentum conservation (again neglecting forces associated with edge effects) implies the two conditions

$$\left. \begin{aligned} 2\langle Y\rangle\sigma^2 &= S_-(t) + S_-\left(t + \tfrac{1}{2}\right) \equiv M_{\text{in}}, \\ S_- &= Y\int_0^1 \left[\left(G + \tfrac{1}{2Y}H_\eta\right)^2 + Re_\omega^{-1}\left(\tfrac{1}{2}\Pi + \tfrac{1}{8}\Gamma + P\right)\right]\mathrm{d}\eta. \end{aligned} \right\} \tag{B 20a}$$

$$2\langle Y\rangle\sigma^2 + p_{-\infty} = S_+(t) + S_+\left(t + \tfrac{1}{2}\right) \equiv M_{\text{out}},$$

$$\left. S_+ = Y \int_0^1 \left[\left(G - \tfrac{1}{2Y}H_\eta\right)^2 - Re_\omega^{-1}\left(\tfrac{1}{2}\Pi - \tfrac{1}{8}\Gamma - P\right)\right]d\eta. \right\} \tag{B 20b}$$

The difference between M_{in} and M_{out} must equal the rate of change of channel momentum (which vanishes upon integration over the channel area, because it is proportional to the mass flux), plus $D(t)$, yielding the relation $\delta p_{-\infty} = -D(t)$. The time dependence of the downstream pressure is a peculiarity of our dealing with a venetian blind which is infinite in y, z. The blind acts as an 'actuator plane' and the instantaneous drag can be balanced only by a pressure difference across the plane.

Thus the momentum balance at each edge provides a way of computing the pressure at the channel edges, but momentum balance provides no new constraint on Π. Since the mass conservation involves simultaneously $q(t)$ and $q(t + 1/2)$, $q(t)$ and therefore Π remain undetermined.

Consider now the use of the outflow principle and the assumption $\delta Re_\omega \gg 1$, leading to the flux function (5.11). We may now solve

$$q - \dot{Y} = -\dot{Y} + q_0 + Re_\omega q_1 + Re_\omega^2 q_2 + O\left(Re_\omega^3\right) \tag{B 21}$$

for Π by inversion of the series. This yields

$$\Pi = \Pi_0 + Re_\omega \Pi_1 + Re_\omega^2 \Pi_2 + O\left(Re_\omega^3\right), \tag{B 22a}$$

$$\Pi_0 = 3Y^{-3}q, \quad \Pi_1 = 3Y^{-3}\left[\frac{2}{15}\dot{\Pi}_0 Y^5 + \frac{8}{105}\Pi_0 \dot{Y}Y^4\right], \tag{B 22b}$$

$$\Pi_2 = 3Y^{-3}\left[\frac{2}{15}\dot{\Pi}_1 Y^5 + \frac{8}{105}\Pi_1 \dot{Y}Y^4 - \frac{17}{315}\ddot{\Pi}_0 Y^7 \right.$$
$$\left. - \left(\frac{53}{315}\dot{Y}\dot{\Pi}_0 - \frac{136}{4725}\ddot{Y}\Pi_0\right)Y^6 - \frac{6421}{121275}\dot{Y}^2\Pi_0 Y^5\right]. \tag{B 22c}$$

To calculate now the drag $D(t)$ per unit length on one slat, recall that

$$D(t) = \frac{1}{Re_\omega}\left[-\frac{1}{Y(t)}G_\eta(1, t) + \frac{1}{Y(t + 1/2)}G_\eta(-1, t + 1/2)\right]$$
$$\equiv \frac{1}{Re_\omega}\left(D_0 + Re_\omega D_1 + Re_\omega^2 D_2 + \dots\right). \tag{B 23}$$

From (B 10) and (B 12a) we obtain

$$D_0 = \Pi Y(t) + \Pi Y(t + 1/2), \tag{B 24a}$$

$$D_1 = -\left[\tfrac{1}{3}\dot{\Pi}Y^3(t) + \tfrac{1}{5}\dot{Y}Y^2\Pi\right](t) - \left[\tfrac{1}{3}\dot{\Pi}Y^3(t) + \tfrac{1}{5}\dot{Y}Y^2\Pi\right](t + 1/2), \tag{B 24b}$$

$$D_2 = \frac{2}{15}\ddot{\Pi}Y^5 + \left(\frac{38}{525}\ddot{Y}\Pi + \frac{44}{105}\dot{Y}\dot{\Pi}\right)Y^4 + \frac{206}{1575}\dot{Y}^2\Pi Y^3. \tag{B 24c}$$

Inserting the functions Π_i from (B 22), and then averaging over time, we obtain (5.27).

REFERENCES

BATCHELOR, G. K. 1967 *An Introduction to Fluid Dynamics.* Cambridge University Press.

BLAKE, J. R. 1971 A spherical envelope approach to ciliary propulsion. *J. Fluid Mech.* **46**, 199–208.

BRENNEN, C. 1975 An oscillating boundary-layer theory for ciliary propulsion. *J. Fluid Mech.* **65**, 799–824.

CHILDRESS, S. 1981*a Mechanics of Swimming and Flying*. Cambridge University Press.

CHILDRESS, S. 1981*b* Physiological fluid dynamics. In *Mathematical Aspects of Physiology* (ed. F. C. Hoppensteadt), pp. 141–163. American Mathematical Society.

CHURCHILL, R. V. 1948 *Introduction to Complex Variables*. McGraw-Hill.

DUDLEY, R. 2000 *The Biomechanics of Insect Flight: Form, Function, Evolution*. Princeton University Press.

DURAND, W. F. 1963 *Aerodynamic Theory*, Vol. II. Dover.

IIMA, M. & YANAGITA, T. 2001 Is a two-dimensional butterfly able to fly by symmetric flapping? *J. Phys. Soc. Japan* **70**, 5–8.

LAMB, H. 1945 *Hydrodynamics*. Dover.

LIGHTHILL, M. J. 1975 *Mathematical Biofluiddynamics*. Society of Industrial and Applied Mathematics, Philadelphia.

JAFFRIN, M. J. & SHAPIRO, A. H. 1971 Peristaltic pumping. *Annu. Rev. Fluid Mech.* **3**, 13–36.

JUNG, E. 1999 2-D simulations of valveless pumping using the immersed boundary method PhD Thesis, Courant institute of Mathematical Sciences, New York University.

JUNG, E. & PESKIN, C. S. 2001 2-D simulations of valveless pumping using the immersed boundary method. *SIAM J. Sci. Comput.* **23**, 19–45.

MCHENRY, M. J., AZIZI, E. & STROTHER, J. A. 2003 The hydrodynamics of locomotion at intermediate Reynolds numbers: undulatory swimming in ascidian larvae (*Botrylloides sp.*) *J. Expl. Biol.* **206**, 327–343.

PURCELL, E. M. 1977 Life at low Reynolds number. *Am. J. Phys.* **45**, 3–11.

WALKER, J. 2002 Functional morphology and virtual models: physical constraints on the design of oscillating wings, fins, legs, and feet at intermediate Reynolds numbers. *Integ. Comput. Biol.* **42**, 232–242.

WANG, Z. J. 2000 Vortex shedding and optimal flapping flight. *J. Fluid Mech.* **410**, 323–341.